drawings illustrating the 10 stages of the teeth as observed radiographically. In addition, Nolla noted that in order to obtain an appraisal of the development of a particular tooth, the radiograph was matched as closely as possible with the comparative figure. When the radiographic reading lay between two grades, this appraisal was indicated with a value of 0.5. For example, if between one-third and two-third of the tooth formation was completed, the reading of the radiograph was given a value of 7.5. When the radiographic value was slightly greater than the illustrated grade, but not as much as half way between that stage and the next, the value 0.2 was added. For example, if slightly more than two-thirds of the crown were completed it would become 4.2, or if somewhat more than one-third of the tooth were completed the grade would become 7.2. In the present study, the authors used Nolla's criteria and the development stages of each permanent tooth in only maxilla on MDCT pantomographs were scored slightly higher than the conventional pantomographs. MDCT pantomographs were clearer at the apical part of permanent teeth than conventional pantomographs, because MDCT pantomographs can confirm the tooth apex by the image in each slice. With regards the difference between maxilla and mandible, the authors considered that the permanent germs in maxilla were complexly located within thick bone, the positions of those germs, however, in mandible were located within thin bone.

Mesiodistal diameter of the crown in each primary and permanent tooth, and upper and lower dental arch widths in MDCT images were close to the corresponding values on the phantom. As the reliabilities of the tooth size and dental arch width measurements on MDCT and on phantom were both high, there were no significant differences in the mean and standard deviation of tooth size and dental arch width between MDCT images and the six phantoms. The measurements of tooth size and dental arch width on MDCT were sufficiently precise for dental structure analyses.

However, helical CT places a high economic and biological burden on the patient because of its high cost and high radiation exposure. As radiation has a cumulative effect on the human body, any reduction in exposure to radiation is considered beneficial. A newly developed type of CT reduces exposure time and simultaneously the absorbed radiation to the patient (13, 14), and MDCT exhibits more reduction of exposure.

Accurate landmarks should be put on images for mesiodistal diameter measurement. In some cases, it was quite difficult to identify the position of the landmark ; however, the mean value was similar to the tooth size on the phantom. The diagnosis of microdontia, macrodontia and abnormality of tooth morphology was reliable in the MDCT images. It was found that the measurements of tooth size and dental arch width on MDCT image were not significantly different from phantom measurements. A slight difference between MDCT data and phantom data does not translate into clinical relevance. The significant differences in this study were similar in magnitude to those of Cavalcanti *et al.* (15), who used cone beam CT. In the present study, most data regarding tooth development stage in each permanent tooth on MDCT pantomographs were significantly larger than those of conventional pantomographs. This finding suggested that the CT pantomograph was clearer and it showed more detail than conventional pantomographs. When MDCT pantomograph is used to evaluate tooth development age in clinics, clinicians have to consider the disagreement from Nolla criteria which based on conventional pantomograph. From this study, it was found that the tooth development stage on MDCT pantomographs was significantly earlier than that on conventional pantomographs, and tooth size and dental arch width on MDCT were similar to those of direct measurement on phantoms using a 1/20 mm caliper.

Conclusion

In this study, the average intraobserver error of tooth development stages in 56 permanent teeth was 0.3, and that of tooth size and dental arch widths on phantoms and MDCT was within 0.6 mm. The tooth

development stages in all permanent teeth were evaluated using conventional and MDCT pantomographs of dry human skulls, and the data of MDCT panoramagraphs were slightly higher than that of conventional pantomographs in only maxilla. The average differences in the mesiodistal diameters of all teeth and dental arch widths between phantoms and MDCT images were less than 0.3 mm, which was not significant.

From this study, the tooth development stage, tooth mesiodistal diameter and dental arch width analyses on MDCT image were found to be clinically precise.

Acknowledgments

The authors are grateful to Prof. T. Kaneda of the Department of Radiology in Nihon University School of Dentistry at Matsudo, valuable advice and Prof. E. Kanazawa of the Department of Anatomy and Physical Anthropology in Nihon University School of Dentistry at Matsudo, for his continuous and kind support.

This study was funded in part by a Grant for the Support of Projects for Strategic Research at Private Universities by the Ministry of Education, Culture, Sports, Science and Technology (MEXT), 2008-2012.

References

1. Nolla CM : The development of the permanent teeth. J Dent Child, 27 : 254-266, 1960.
2. Liversidge HM : Permanent tooth formation as a method of estimating age. Front Oral Biol, 13 : 153-157, 2009.
3. Moyer RE. Handbook of orthodontics. Analysis of the dentition and occlusion. 4th ed. Year Book Medical Publishers ; 1988. p.235-238.
4. Jones KL : Smith's recognizable patterns of human malformation, 4th edition 1988 WB Saunders Company, Philadelphia, USA.
5. Broadbent BH : A new technique and its application to orthodontia. Angle Orthod, 1 : 45-66, 1931.
6. Gottlieb EL, Nelson AH, Vogels DS : 1990 JCO study of orthodontic diagnosis and treatment procedures. 1. Results and trends. J Clin Orthod, 25 : 145-156, 1991.
7. Nakayama E, Sugiura K, Ishibashi H, Oobu K, Kobayashi I, Yoshiura K : The clinical and diagnostic imaging findings of osteosarcoma of the jaw. Dentomaxillofac Radiol, 34 : 182-188, 2005.
8. Dos Santos DT, Costa e Silva APA, Vannier MW, Cavalcanti MGP : Validty of multislice computerized tomography for diagnosis of maxillofacial fractures using an independent workstation. Oral Surg Oral Med Oral Pathol Oral Radiol Endod, 98 : 715-720, 2004.
9. Mahasantipiya PM, Savage NW, Monsour PAJ, Wilson RJ : Narrowing of the inferior dental canal in relation to the lower third molars. Dentomaxilofac Radiol, 34 : 154-163, 2005.
10. Flohr TG, Schaller S, Stierstorfer K, Bruder H, Ohnesorge BM, Schoepf UJ : Multi-detector row CT systems and image-reconstruction techniques. Radiology, 235 : 756-773, 2005.
11. Jaffe TA, Nelson RC, Johnson GA, Lee ER, Yoshizumi TT, Lowry CR, Bullard AB, Delong DM, Paulson EK : Optimization of multiplanar reformations from isotropic data sets acquired with 17-detector row helical CT scanner. Radiology, 238 : 292-299, 2006.
12. Erasmus JJ, Gladish GW, Broemeling L, Sabloff BS, Truong MT, Herbst RS, Munden RF : Interobserver and intraobserver variability in measurement of non-small-cell carcinoma lung lesions : implications for assessment of tumor response. J Clin Oncol, 21 : 2574-2582, 2003.
13. Mozzo P, Procacci C, Tacconi A, Martini PT, Andreis IA : A new volumetric CT machine for dental imaging based on the cone-beam technique : preliminary results. Eur Radiol, 8 : 1558-1564, 1998.
14. Mah JK, Danforth RA, Bumann A : Radiation absorbed in maxillofacial imaging with a new dental computed tomography device. Oral Surg Oral Med Oral Pathol Oral Radiol Endod, 96 : 508-513, 2003.
15. Cavalcanti MG, Vannier MW : Three dimensional computed tomography landmark measurement in craniofacial surgical planning : experimental validation in vitro. J Oral Maxillofac Surg, 57 : 690-694, 1999.

RAPID PUBLICATION

AMERICAN JOURNAL OF medical genetics PART A

A New Ehlers–Danlos Syndrome With Craniofacial Characteristics, Multiple Congenital Contractures, Progressive Joint and Skin Laxity, and Multisystem Fragility-Related Manifestations

Tomoki Kosho,[1]* Noriko Miyake,[2] Atsushi Hatamochi,[3] Jun Takahashi,[4] Hiroyuki Kato,[4] Teruyoshi Miyahara,[5] Yasuhiko Igawa,[6] Hiroshi Yasui,[7] Tadao Ishida,[7] Kurahito Ono,[8] Takashi Kosuda,[9] Akihiko Inoue,[10] Mohei Kohyama,[11] Tadashi Hattori,[12] Hirofumi Ohashi,[13] Gen Nishimura,[14] Rie Kawamura,[1] Keiko Wakui,[1] Yoshimitsu Fukushima,[1] and Naomichi Matsumoto[2]

[1]Department of Medical Genetics, Shinshu University School of Medicine, Matsumoto, Japan

[2]Department of Human Genetics, Yokohama City University Graduate School of Medicine, Yokohama, Japan

[3]Department of Dermatology, Dokkyo Medical University, School of Medicine, Mibu, Japan

[4]Department of Orthopedics, Shinshu University School of Medicine, Matsumoto, Japan

[5]Department of Ophthalmology, Shinshu University School of Medicine, Matsumoto, Japan

[6]Department of Urology, Shinshu University School of Medicine, Matsumoto, Japan

[7]First Department of Internal Medicine, Sapporo Medical University, Sapporo, Japan

[8]Department of Orthopedics, Tomioka General Hospital, Tomioka, Japan

[9]Department of Pediatrics, Tomioka General Hospital, Tomioka, Japan

[10]Department of Surgery, Tomioka General Hospital, Tomioka, Japan

[11]Department of Surgery, JA Hiroshima General Hospital, Hiroshima, Japan

[12]Department of Orthopedics, Aichi Children's Health and Medical Center, Oobu, Japan

[13]Division of Medical Genetics, Saitama Children's Medical Center, Saitama, Japan

[14]Department of Radiology, Tokyo Metropolitan Kiyose Children's Hospital, Kiyose, Japan

Received 27 January 2010; Accepted 13 April 2010

We previously described two unrelated patients showing characteristic facial and skeletal features, overlapping with the kyphoscoliosis type Ehlers–Danlos syndrome (EDS) but without lysyl hydroxylase deficiency [Kosho et al. (2005) Am J Med Genet Part A 138A:282–287]. After observations of them over time and encounter with four additional unrelated patients, we have concluded that they represent a new clinically recognizable type of EDS with distinct craniofacial characteristics, multiple congenital contractures, progressive joint and skin laxity, and multisystem fragility-related manifestations. The patients exhibited strikingly similar features according to their age: *craniofacial*, large fontanelle, hypertelorism, short and downslanting palpebral fissures, blue sclerae, short nose with hypoplastic columella, low-set and rotated ears, high palate, long philtrum, thin vermilion of the upper lip, small mouth, and micro-retrognathia in infancy; slender and asymmetric face with protruding jaw from adolescence; *skeletal*, congenital contractures of fingers, wrists, and hips, and talipes equinovarus with anomalous insertions of flexor muscles; progressive joint laxity with recurrent dislocations; slender and/or cylindrical fingers and

Additional supporting information may be found in the online version of this article.

Grant sponsor: Research on Intractable Diseases, Ministry of Health, Welfare, and Labor, Japan; Grant Number: #2141039040; Grant sponsor: Shinshu Association for the Advancement of Medical Sciences; Grant sponsor: Grant-in-Aid for Exploratory Research of Young Scientists, Shinshu University.

*Correspondence to:
Tomoki Kosho, M.D., Department of Medical Genetics, Shinshu University School of Medicine, 3-1-1 Asahi, Matsumoto 390-8621, Japan.
E-mail: ktomoki@shinshu-u.ac.jp

Published online 14 May 2010 in Wiley InterScience
(www.interscience.wiley.com)
DOI 10.1002/ajmg.a.33498

© 2010 Wiley-Liss, Inc.

progressive talipes valgus and cavum or planus, with diaphyseal narrowing of phalanges, metacarpals, and metatarsals; pectus deformities; scoliosis or kyphoscoliosis with decreased physiological curvatures of thoracic spines and tall vertebrae; *cutaneous*, progressive hyperextensibility, bruisability, and fragility with atrophic scars; fine palmar creases in childhood to acrogeria -like prominent wrinkles in adulthood, recurrent subcutaneous infections with fistula formation; *cardiovascular*, cardiac valve abnormalities, recurrent large subcutaneous hematomas from childhood; *gastrointestinal*, constipation, diverticula perforation; *respiratory*, (hemo)pneumothorax; and *ophthalmological*, strabismus, glaucoma, refractive errors. © 2010 Wiley-Liss, Inc.

Key words: a new type Ehlers–Danlos syndrome; craniofacial characteristics; multiple congenital contractures; joint laxity; talipes deformities; kyphoscoliosis; skin laxity; multisystem fragility; recurrent subcutaneous hematomas

How to Cite this Article:
Kosho T, Miyake N, Hatamochi A, Takahashi J, Kato H, Miyahara T, Igawa Y, Yasui H, Ishida T, Ono K, Kosuda T, Inoue A, Kohyama M, Hattori T, Ohashi H, Nishimura G, Kawamura R, Wakui K, Fukushima Y, Matsumoto N. 2010. A new Ehlers–Danlos syndrome with craniofacial characteristics, multiple congenital contractures, progressive joint and skin laxity, and multisystem fragility-related manifestations.
Am J Med Genet Part A 152A:1333–1346.

INTRODUCTION

The Ehlers–Danlos syndrome (EDS) is a heterogeneous group of heritable connective tissue disorders affecting as many as 1 in 5,000 individuals, characterized by joint and skin laxity, and tissue fragility [Steinmann et al., 2002]. The fundamental mechanisms of EDS are known to consist of dominant-negative effects or haploinsufficiency of mutant procollagen α-chains and deficiency of collagen-processing-enzymes [Mao and Bristow, 2001]. In a revised nosology, Beighton et al. [1998] classified EDS into six major types: (1) classical type (OMIM#130000) (causative gene, *COL5A1* or *COL5A2*; affected protein, α1(V) or α2(V) procollagen), (2) hypermobility type (OMIM#130020) (*TNXB*; tenascin-XB, in a small subset of cases), (3) vascular type (OMIM#130050) (*COL3A1*; α1(III) procollagen), (4) kyphoscoliosis type (OMIM#225400) (*PLOD*; lysyl hydroxylase), (5) arthrochalasia type (OMIM#130060) (*COL1A1* or *COL1A2*; α1(I) or α2(I) procollagen), and (6) dermatospraxis type (OMIM#225410) (*ADAMTS2*; procollagen I N-proteinase). Additional minor variants of EDS have been identified with molecular and biochemical abnormalities: Brittle cornea syndrome (OMIM#229200) (*ZNF469*) [Abu et al., 2008], EDS-like syndrome due to tenascin-XB deficiency (OMIM#606408) (*TNXB*; tenascin-XB) [Schalkwijk et al., 2001], progeroid form (OMIM#130070) (*β4GALT7*; xylosylprotein 4-beta-galactosyltransferase) [Kresse et al., 1987], cardiac valvular form (OMIM#225320) (*COL1A2*; α2(I) procollagen) [Schwarze et al., 2004], and EDS-like spondylocheirodysplasia (OMIM#612350) (*SLC39A13*; a membrane-bound zinc transporter) [Giunta et al., 2008].

We previously described two unrelated patients showing characteristic facial and skeletal features, with similarities to kyphoscoliosis type EDS but without lysyl hydroxylase deficiency [Kosho et al., 2005]. After observations of them over time and encounter with four additional unrelated patients including one reported by Yasui et al. [2003], we have concluded that they represent a new clinically recognizable type of EDS characterized by distinct craniofacial features, multiple congenital contractures, progressive joint and skin laxity, and progressive multisystem complications associated with tissue fragility including recurrent large subcutaneous hematomas. Here, we present detailed clinical courses of the six patients to delineate the disorder.

CLINICAL REPORTS

Patient 1

The patient is a now 16-year-old Japanese girl. Part of her history was described previously [Kosho et al., 2005]. She was the first child of a healthy mother and a healthy non-consanguineous father, both 19 years of age. She was born by normal vaginal delivery at 42 weeks of gestation. Her birth weight was 2,724 g (−1.3 SD), length 50.0 cm (−0.1 SD), and OFC 32.5 cm (−1.0 SD). She was admitted for the treatment of hypoglycemia, hyperbilirubinemia, and left talipes equinovarus (Fig. 1J). Her craniofacial features included a large fontanelle, hypertelorism, short and downslanting palpebral fissures, blue sclerae, a short nose with a hypoplastic columella, low-set and rotated ears, a high palate, a long philtrum, a thin upper lip vermilion, a small mouth, and micro-retrognathia (Fig. 1A). She had arachnodactyly, flexion-adduction contractures of bilateral thumbs, flexion contractures of the metacarpophalangeal (MP) and interphalangeal (IP) joints in the other fingers (Fig. 1E,F), and rigidity of bilateral hip joints. She suckled poorly, and was admitted again for the treatment of dehydration at age 1 month. Talipes equinovarus was treated with serial plaster casts, and was surgically corrected at age 2 years. Anomalous insertions of the flexor muscles were observed at the operation. Gross motor development was delayed: she sat at age 10 months and walked unassisted at age 2 years. Her skin was easily torn, but showed normal hemostasis in open wounds. Her face became longer with bushy and arched eyebrows and a pointed chin (Fig. 1B). At age 4 years, she developed a large subcutaneous hematoma over the occiput after falling, followed by acute hemorrhagic anemia that required admission and transfusion of hemostatic agents and packed red cells. During the admission, she was suspected to have EDS. At age 6 years, she developed a large subcutaneous hematoma over the temporo-occipital region after falling, requiring admission and intravenous administration of hemostatic agents. She had recurrent dislocations of the shoulders, elbows, and knees.

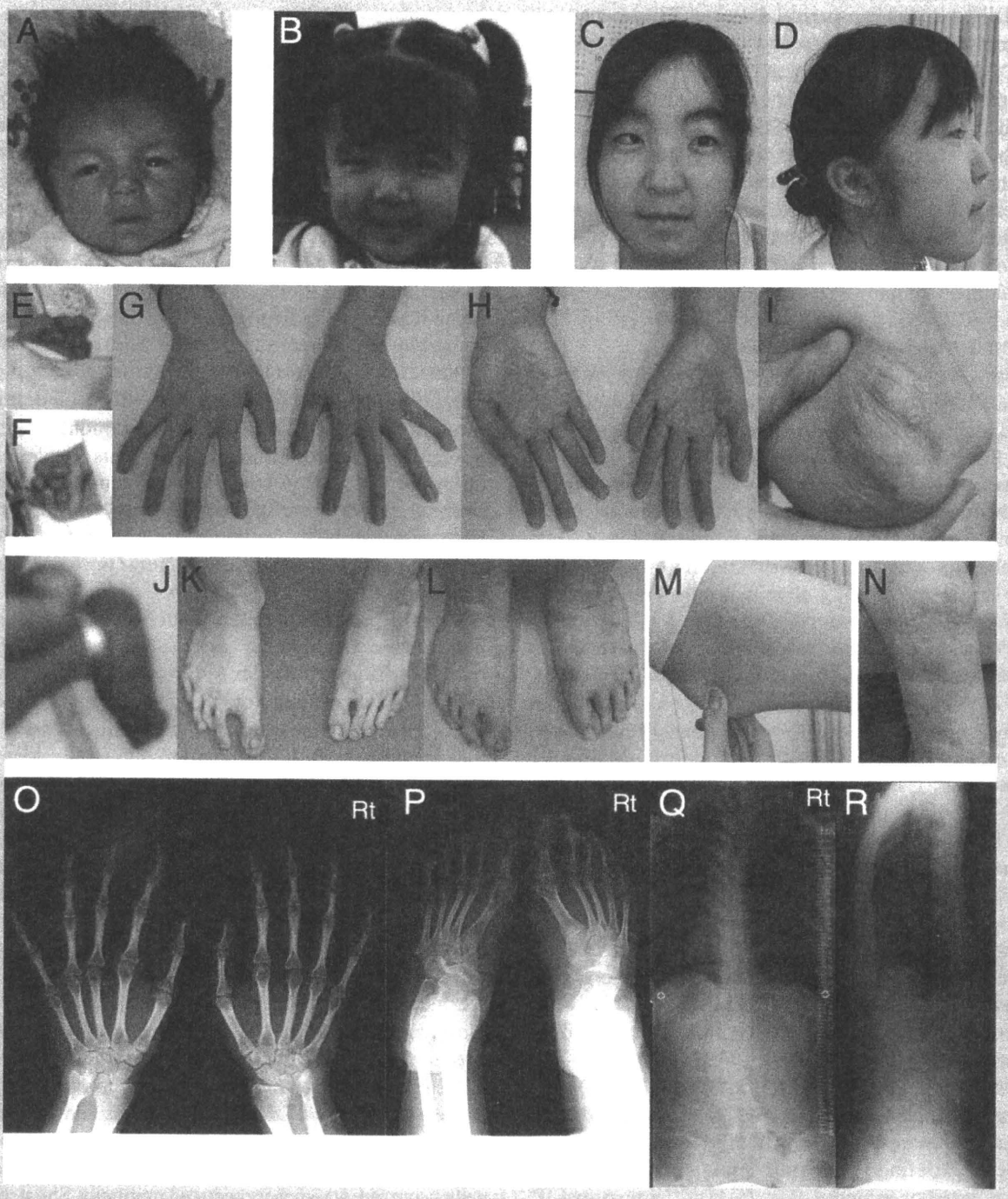

FIG. 1. Patient 1. Clinical photographs of the face at age 23 days (A), 3 years (B), and 16 years (C,D); the left (E) and the right (F) hands at age 23 days; the hands at age 16 years (G,H); the left elbow at age 16 years (I); the feet at birth (J), age 11 years (K), and 16 years (L); the skin on the left upper arm at age 16 years (M); and the left knee at age 16 years (N). Radiographs of the hands (O), the feet (P), and the spine (Q,R) at age 16 years. [Color figure can be viewed in the online issue, which is available at www.interscience.wiley.com.]

When first seen by us at age 7 years, she weighed 19.2 kg (−1.0 SD), height 123.8 cm (+0.8 SD), and OFC 51.5 cm (±0 SD). She had generalized joint laxity, a straight back with scoliosis, and cylindrical and slender fingers. Her skin was hyperextensible, bruisable, and fragile with multiple atrophic scars. Hyperalgesia to pressure such as measuring blood pressure at the upper arms was noted. Ophthalmological examinations showed microcornea and hyperopia. Otological examinations showed narrow middle ear spaces and hearing impairment of high-pitched sounds. Heart murmurs were not audible, and cardiac ultrasonography showed trivial mitral valve regurgitation. Her bladder was dilated with urinary retention and frequent cystitis, requiring manual pressure

voiding. She developed a large subcutaneous hematoma over the buttock after falling, requiring surgical drainage. Treatment with temporary intranasal administration of 1-desamino-8-D-arginine vasopressin (DDAVP) after injuries was started.

At age 11 years, she weighed 29.5 kg (−2 SD), height 148.1 cm (+0.2 SD), and OFC 54 cm (+0.2 SD). She had a slender face and a Marfanoid habitus with pectus excavatum and progressing talipes valgus and planus (Fig. 1K). Fine palmar creases and a ganglion on the left foot were noted. Hyperopia had improved and frequency of otitis media had decreased. Urinary retention persisted but manual pressure voiding was not necessary. Heart murmurs were audible, and cardiac ultrasonography showed moderate tricuspid valve regurgitation, prolapse of the tricuspid and mitral valves, and left-to-right shunt via a small atrial septal defect.

At age 12 years, menarche occurred. Kyphoscoliosis progressed with lumbago, necessitating a brace. The ganglion on the left foot was punctured and jellylike contents were suctioned, but soon it swelled again. Persistent urinary incontinence occurred, and urological examinations showed involuntary contractions and hypesthesia of the bladder with normal voiding function. She developed a large subcutaneous hematoma around the head and face after hitting the forehead on a door mirror, with a decline of hemoglobin concentration from 13.4 to 7.7 g/dl in several hours, and was admitted in an intensive care unit (ICU).

She had severe constipation (defecation once a week) and sometimes diarrhea (after having oily or watery foods), treated by medication of *Lactobaccilus* and lactulose from age 15 years. Large bowel sounds resembling a frog-croak were frequently heard. At age 16 years, acute gastric ulcer occurred in the antrum, leading to massive hematemesis. Gastric obstruction soon progressed, and treatment with a proton pump inhibitor and intravenous hyperalimentation (IVH) was not effective. A large thrombus developed at the site of inserting an IVH catheter, and an inferior vena cava filter was placed. Distal gastrectomy with Billroth I reconstruction was performed, complicated by a massive hematoma in the rectus sheath necessitating intranasal administration of DDAVP and transfusion of packed red cells and fresh frozen plasma. She attended a class for handicapped children from her junior high school days due to her physical fragility and mild learning disability.

When last seen by us at age 16 years, she weighed 49.4 kg (−0.4 SD), height 159.2 cm (+0.3 SD), and OFC 55.8 cm (+0.2 SD). Her face was slender with a protruding jaw (Fig. 1C,D). She suffered from lumbago because of progressive kyphoscoliosis. The distal IP joints in bilateral index to little fingers and the IP joints in bilateral thumbs could hardly be flexed or extended (Fig. 1G,H). The proximal IP joints in bilateral index to little fingers and the MP joints in all fingers could be flexed and extended, but could not be moved separately and smoothly (see supporting information Video 1 which may be found in the online version of this article). She had chronic dislocations of bilateral distal radio-ulnar joints and radial heads. Bilateral talipes valgus and planus progressed with extremely soft subcutaneous tissues at the heels (Fig. 1L), resulting in difficulty in walking. The IP joints in bilateral toes could not be moved and metatarsophalangeal joints could only be moved slightly. She had skin redundancy (Fig. 1M) and fragility with atrophic scars (Fig. 1N), fine palmar creases (Fig. 1H), and recurrent subcutaneous infections at the elbows (Fig. 1I) and the buttocks with fistula formation.

Patient 2

The patient is a now 32-year-old Japanese woman. Part of her history was described previously [Kosho et al., 2005]. She was born at term as the third child of a healthy 27-year-old mother and a healthy 37-year-old father, who were first cousins once removed. Her birth weight was 2,500 g (−2 SD) and two elder sisters were healthy. She suckled poorly, and was gavage fed for the first week of life. At age 9 weeks, she was admitted for the treatment of multiple contractures. Her craniofacial features included a large anterior fontanelle, hypertelorism, strabismus, short and downslanting palpebral fissures, a short nose with a hypoplastic columella, low-set and rotated ears, a long philtrum, a thin upper lip vermilion, a high palate, and micro-retrognathia (Fig. 2A). Skeletal features included extension contractures with ulnar deviation of bilateral wrists, flexion-adduction contractures of bilateral thumbs, flexion contractures of the MP joints in bilateral middle to little fingers, extension contractures of the distal IP joints in bilateral index to little fingers (Fig. 2E,F), bilateral talipes equinovarus (Fig. 2I), and a congenital dislocation of the right hip. Active movement of her fingers was poor. Mild skin hyperextensibility was noted. Talipes equinovarus and finger-wrist contractures were treated with serial plaster casts.

At age 1 year and 2 months, she underwent surgical corrections of bilateral talipes equinovarus. Anomalous insertions of the flexor muscles (the tibialis posterior to the talus [normal, navicular and cuneiform bones], the flexor digitorum longus to the abductor hallucis muscle [normal, bases of distal phalanges of four lesser toes], and the flexor hallucis longus to the calcaneus [normal, base of distal phalanx of hallux]) (Fig. 3) were shown to cause talipes equinovarus and inability to flex toes. Tendon sheaths of the muscles were hypoplastic, and surrounding tissues were fragile and hyperextensible. Skin hyperextensibility became more evident with frequent bruises. At age 2 years, dislocation of the right hip was treated through overhead traction and manual reduction under general anesthesia. Her tentative clinical diagnosis was Freeman–Sheldon syndrome.

Gross motor development was delayed: she raised her head at age 4 months, sat unassisted at 7 months, stood up assisted at 2 years and 6 months, cruised furniture at 3 years, and waked alone with short leg braces at 5 years. Generalized hypotonia and joint laxity became evident, and bilateral talipes valgus and cavus progressed (Fig. 2J). Her face became longer with drooping eyelids and bushy eyebrows (Fig. 2B). At age 6 years, dislocations of the left hip and the patella occurred, which were reduced manually. She also developed a subcutaneous hematoma around the left knee that required surgical drainage. She had constipation, and from incontinence and recurrent urinary tract infections associated with an atonic bladder and urinary retention. She had visual impairment from myopia and astigmatism, and impaired hearing for high-pitched sounds. At age 8 years, she developed a wound on the buttocks after falling, followed by bacterial infections and fistula formation, which lead to skin defects including decubitus necessitating plastic surgery. At age 11 years, she fell and developed a large subcutaneous hematoma over the head, requiring surgical drainage and transfusion of packed red cells. At age 12 years, she had dislocation of the left patella and left shoulder after minor injuries, which were

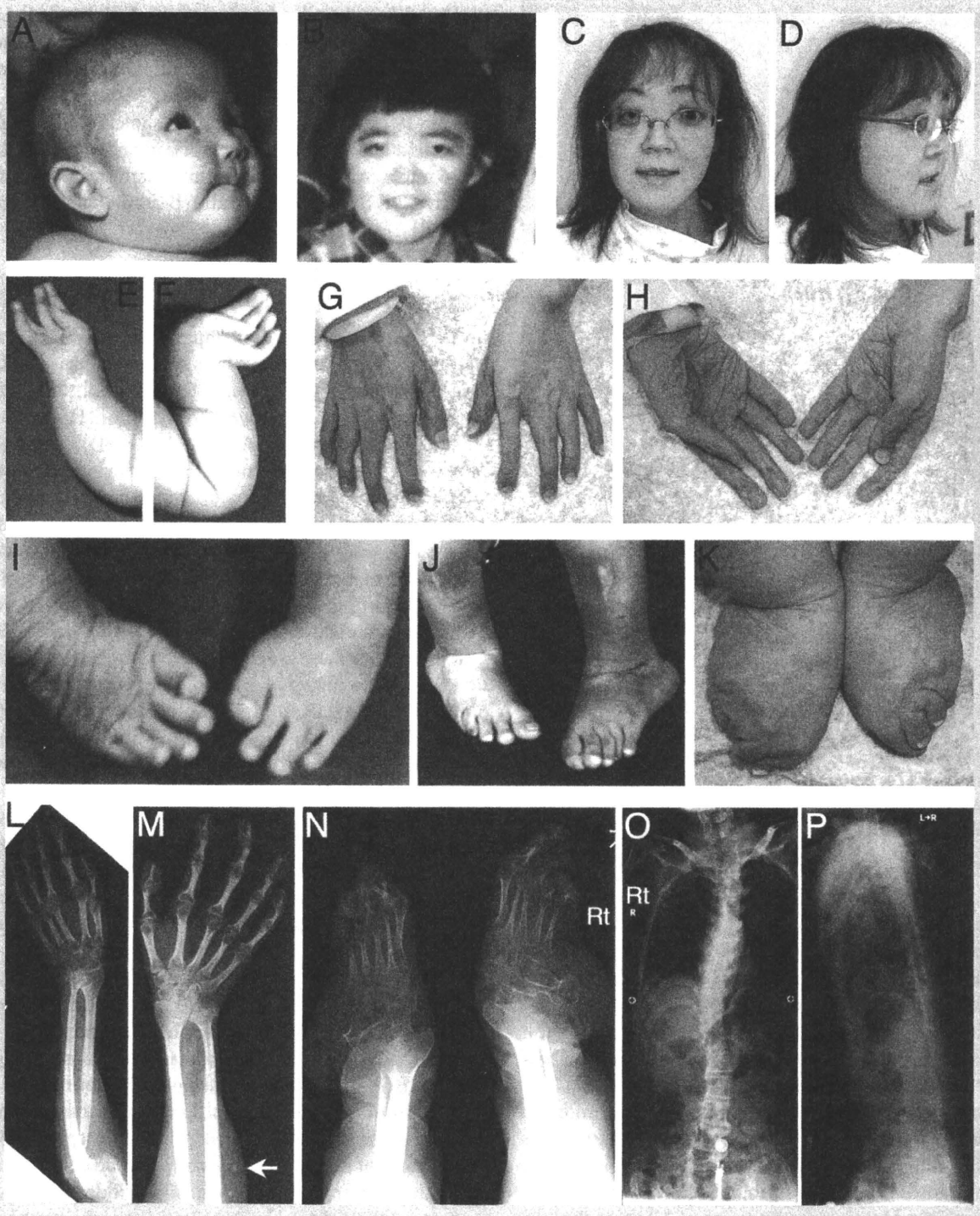

FIG. 2. Patient 2. Clinical photographs of the face at age 3 months (A), 8 years (B), and 28 years (C,D); the right arm at age 2 months (E); the left arm at age 3 months (F); the hands at age 28 years (G,H); and the feet at age 2 months (I), 6 years (J), and 28 years (K). Radiographs of the left (L) and the right (M) arms, the feet (N), and the spine (O,P) at age 28 years. An arrow indicates ectipic calcification (M). [Color figure can be viewed in the online issue, which is available at www.interscience.wiley.com.]

reduced manually. Her IQ was normal at 99. She attended a school for handicapped children because of limitations of daily activities bound to a wheelchair. Her clinical diagnosis was confirmed as EDS. At age 15 years, her height was 140 cm (−3.2 SD). She had marked muscle weakness with grip power 5 kg in the right and 2 kg in the left. She became exhausted easily. Frequent dislocations of the shoulders and elbows were reduced manually by her. Scoliosis was also noted.

At age 24 years, she underwent surgery for colonic perforation associated with diverticulitis. At the operation, multiple colonic

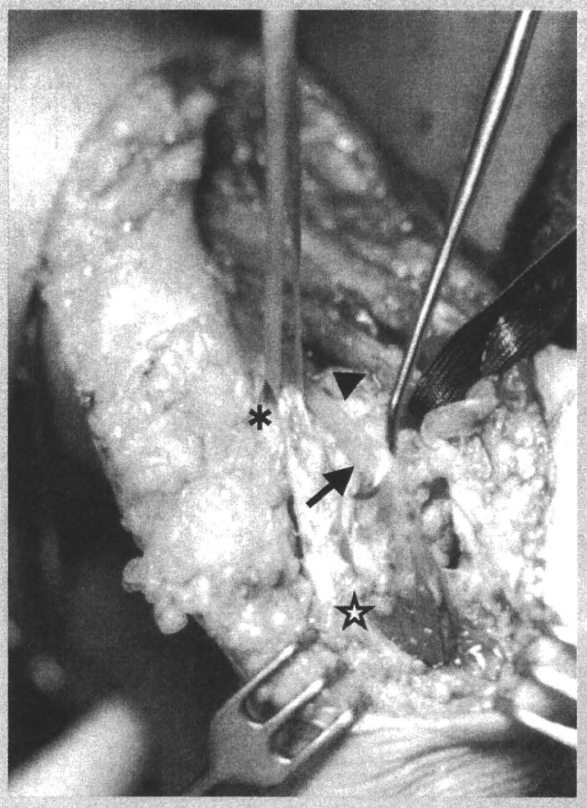

FIG. 3. An operative finding at postero-medial release in the right foot of Patient 2. Anomalous insertions of the flexor muscles are noted: the tibialis posterior muscle (*) to the talus, the flexor digitorum longus muscle (arrow) to the abductor hallucis muscle (blank star), and the flexor hallucis longus muscle (arrowhead) to the calcaneus.

diverticula were observed. At age 26 years, visual impairment progressed due to bilateral glaucoma with an elevation of intraocular pressure (IOP) to 20 mmHg in the right eye and 21 mmHg in the left eye, accompanied by a decreased visual field. At age 28 years, she suffered from a right pneumothorax, treated with chest tube drainage. Acute cystitis also occurred, and cystolithiasis was detected in the follow-up ultrasonography.

When seen by us at age 28 years, she was wheelchair-bound. She had a slender face with a protruding jaw (Fig. 2C,D). Her thorax was flat and thin. Her fingers were cylindrical. She had mild flexion contractures of the distal IP joints in bilateral index to little fingers, mild flexion-adduction contractures of bilateral thumbs (Fig. 2G,H), and chronic dislocations of bilateral distal radio-ulnar joints and the left radial head accompanied by ruptured tendon of the extensor pollicis longus muscle. She also had talipes valgus and cavus with extremely soft subcutaneous tissues at the heels (Fig. 2K). She could rarely flex or extend the left thumb or all toes. Her skin was redundant, bruisable, and fragile with atrophic scars. Prominent wrinkles in the palms showed acrogeria (Fig. 2H). She showed hyperalgesia to pressure such as measuring blood pressure at the upper arms. She had chronic subcutaneous abscesses with fistula formation at the elbows and buttocks. She suffered form severe constipation (defecation once a week) requiring oral laxatives and *Lactobaccilus*, but sometimes had diarrhea. Large bowel sounds resembling a frog-croak were frequently heard. Cardiac ultrasonography showed no structural or functional abnormalities in the mitral or aortic valve.

When last seen by us at age 31 years, she suffered from progressive visual field loss, although IOP was controlled within the range of 14–16 mmHg through topical administration of a prostaglandin F2 α derivative (latanoprost) and a β-adrenergic receptor blocker (timolol).

Patient 3

The patient, now a 32-year-old Japanese man, was the first child of a healthy 31-year-old mother and a healthy 25-year-old father, who were first cousins. His younger sister was healthy. He was delivered by vacuum extraction at 40 weeks of gestation. His birth weight was 3,300 g (+0.5 SD), length 52.0 cm (+1.3 SD), and OFC 35.0 cm (+0.8 SD). He was admitted for the treatment of orthopedic complications. He had a triangular face with a large skull, a large anterior fontanelle, hypertelorism, short and downslanting palpebral fissures, strabismus, a short nose with a hypoplastic columella, low-set and rotated ears, a long philtrum, a thin upper lip vermilion, a small mouth, and micro-retrognathia (Fig. 4A). His skeletal features included extension contractures of bilateral wrists, flexion -adduction contractures of bilateral thumbs, flexion contractures of the MP joints in bilateral index to little fingers, of the proximal IP joints in the right index and middle fingers, and of the distal IP joint in the left middle finger; extension contractures of the other IP joints (Fig. 4D,E), rigidity of bilateral hip joints, and bilateral talipes equinovarus (Fig. 4H). His skin was redundant with a lot of creases (Fig. 4D,E). Widely spaced nipples and bilateral cryptorchidism were noted. He was diagnosed as arthrogryposis. Talipes equinovarus was treated with serial plaster casts, and was surgically corrected at age 1 year and 8 months. He also underwent tendon transplantations for defects of tendons to bilateral thumbs, and orchiopexy.

At age 6 years, he developed a subcutaneous hematoma over the buttocks after falling, followed by bacterial infections and fistula formation. At age 8 years, a large subcutaneous hematoma occurred spontaneously over the head and progressed acutely with loss of consciousness, treated with emergency surgical drainage and transfusion of packed red cells. Large subcutaneous hematomas occurred in the left elbow at age 11 years, on the right shin followed by a rupture of another vessel, which spread the hematoma from the thigh to the ankle and made him bedridden for a month at age 14 years; on the right ankle necessitating admission at age 19 years, on the left arm making him bedridden for 2 months at age 26 and 27 years, and on the right shin making him bedridden for 2 months at age 29 years. He also suffered from recurrent joint dislocations of the right knee twice at age 9–10 years and the left shoulder five times at age 22–27 years. He was admitted for the treatment of bronchitis, leading to hearing impairment. At age 29 years, a rupture of a small intestine diverticulum was treated with emergency surgery.

When referred to us at age 30 years, his weight was 45 kg (−1.7 SD) and height 178 cm (+1.2 SD). He could walk independently but used a wheelchair when he went out. He had a skull with a

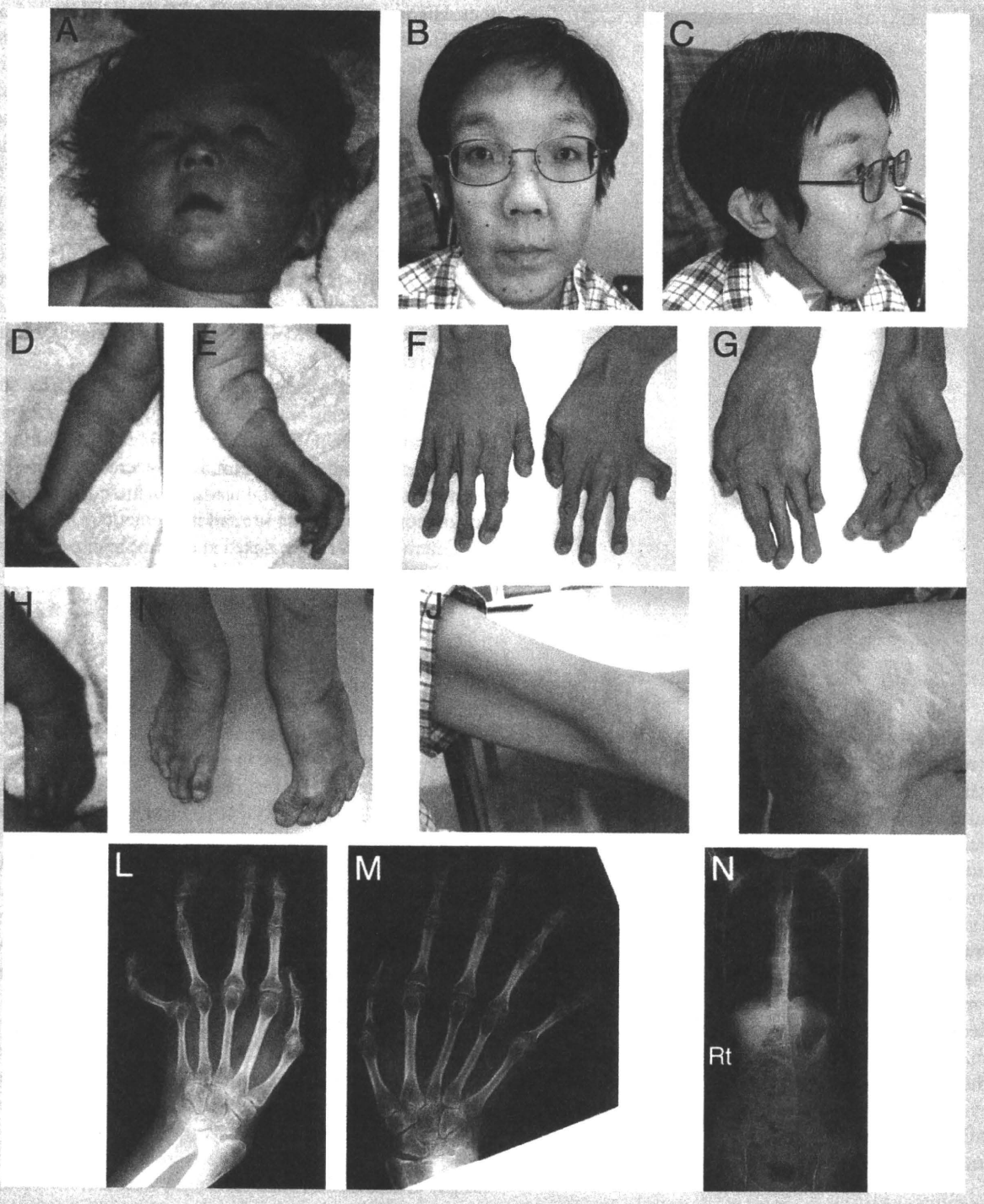

FIG. 4. Patient 3. Clinical photographs of the face in the neonatal period (A) and at age 30 years (B,C); the right (D) and the left (E) arms in the neonatal period; the hands at age 30 years (F,G); the left foot in the neonatal period (H); the feet at age 30 years (I); the skin on the left upper arm at age 30 years (J); and the left knee at age 30 years (K). Radiographs of the left (L) and the right (M) hands, and the spine (N) at age 31 years. [Color figure can be viewed in the online issue, which is available at www.interscience.wiley.com.]

prominent occiput and a lot of white hair, and a slender and asymmetric face with hypertelorism, strabismus, blue sclerae, a short nose with a hypoplastic columella, low-set rotated ears, a long philtrum, a thin upper lip vermilion, a high palate, crowded teeth, and a protruding jaw (Fig. 4B,C). He had a Marfanoid habitus with a flat and thin thorax and kyphoscoliosis. His fingers were slender and cylindrical. He had contractures of fingers and toes with limited flexion or extension (Fig. 4F,G,I), chronic dislocations of bilateral distal radio-ulnar joints and radial heads, and progressive talipes valgus and planus with extremely soft subcutaneous tissues at the

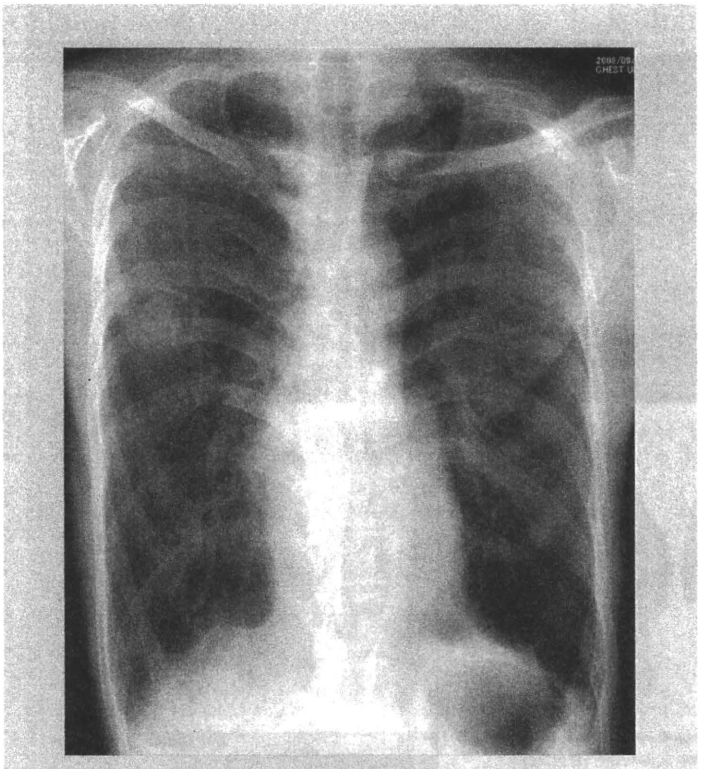

FIG. 5. A chest radiograph of Patient 4 at age 31 years.

heels (Fig. 4I). His skin was redundant (Fig. 4J), bruisable, and fragile with atrophic scars (Fig. 4K). Prominent palmar wrinkles showed acrogeria (Fig. 4G). He showed hyperalgesia to pressure such as measuring blood pressure at the upper arms. He suffered from constipation requiring oral laxatives and *Lactobaccilus*, but sometimes had diarrhea. Large bowel sounds resembling a frog croak were frequently heard. Cardiac ultrasonography showed grade 2 aortic valve regurgitation without dilation of the ascending aorta, and a trace of mitral valve regurgitation. Oththalmological examinations showed microphthalmia, myopia, and astigmatism. He showed hypogonadism without voice changes.

When last seen by us, his physical condition had deteriorated. He was bedridden, because of recurrent subcutaneous large hematomas around the buttocks and thighs possibly caused by spontaneous rupture of vessels or muscles. He also suffered from a dislocation of the right hip joints after falling, followed by another large hematoma throughout the right leg.

Patient 4

The patient is a now 32-year-old Japanese man. Part of his clinical course was described previously [Yasui et al., 2003]. He underwent surgery for bilateral talipes equinovarus at age 1 year. He was diagnosed as EDS at age 4 years. He had six operations for bilateral retinal detachment from age 16 years, and had surgery for carpal tunnel syndrome at age 18 years. Talipes valgus and planus was noticed at age 6 years, and progressed. He wore special orthopedic shoes from age 9 years and underwent surgical fixations of bilateral ankle joints at age 22 years.

At age 23 years, he was admitted for surgical fixation of the left toes. His weight was 38.0 kg (−2.4 SD) and height 168.5 cm (−0.4 SD). He had mild excavation of the left thorax and mildly hyperextensible skin with bruisability. During the preoperative evaluation, prolonged bleeding time was noticed (11 min [normal, 1–5]). He developed a large subcutaneous hematoma over the buttocks after a mild injury, with a decline of hemoglobin concentration from 9.2 to 4.9 g/dl. The hematoma was not resorbed with intranasal DDAVP and intravenous carbazochrome sodium sulfate, tranexamic acid, and packed red cells. It took 9 months for resorption of the hematoma after a combined therapy of daily intranasal DDAVP and weekly intramuscular conjugated estrogen. At age 31 years, he suffered from a right hemopneumothorax with a large bulla, which was treated with chest tube drainage and transfusion of packed red cells.

When last seen by us at age 31 years, his hemostatic condition was controlled by weekly oral doses of conjugated estrogen and temporary intranasal DDAVP after injuries. He had a slender and asymmetric face with hypertelorism, blue sclerae, a high palate, and a protruding jaw. His skeletal features included slender fingers with flexion contractures and limited movements, chronic dislocations of bilateral radial heads, flexed and immobile toes, kyphoscoliosis, and talipes valgus and planus with difficulty in walking. Acrogeria-like palmar wrinkles were noted.

Patient 5

The patient, now a 20-year-old Japanese woman, was the first child of a healthy 24 year-old mother and a healthy 25-year-old father. She was delivered by cesarean section for a breech presentation at 39 weeks of gestation. Her birth weight was 2,800 g (−0.4 SD), length 47.0 cm (−1.1 SD), and OFC 35.0 cm (+1.0 SD). She exhibited apnea with severe cyanosis on the day of her birth, and was admitted to a neonatal ICU. Her craniofacial features included a large anterior fontanelle, hypertelorism, short and downslanting palpebral fissures, strabismus, a short nose with a hypoplastic columella, a long philtrum, a thin upper lip vermilion, a small mouth, a high palate, and micro-retrognathia. Her skeletal features included pectus excavatum, slender fingers with flexion-adduction contractures of bilateral thumbs and extension contractures in bilateral index to little fingers (Fig. 6A), and bilateral talipes equinovarus (Fig. 6C,D). She hated to be hugged tightly. Bilateral talipes equinovarus were treated with serial plaster casts, followed by surgical corrections at age 1 year. At the operation, anomalous insertions of the flexor muscles were noted: the flexor digitorum longus and the flexor hallucis longus were not inserted to the toes, but were fused in the soles, forming a fascia-like tissue. Bilateral hip dislocations were treated by a brace, followed by a surgical correction in the right hip. Her skin was easily bruised and torn after a mild injury. Recurrent joint dislocations occurred easily or spontaneously at the elbows, shoulders, and knees. Constipation was treated with glycerin enema, and then improved with drinking milk or coffee after age 2 years. She raised her head at age 8 months, sat unassisted at age 1 year, and walked independently at age 2 years and 2 months. She was suspected to have EDS at around age 5 years.

She developed large subcutaneous hematomas over the buttocks after falling at age 6 years and age 7 years. At age 9 years, she suffered

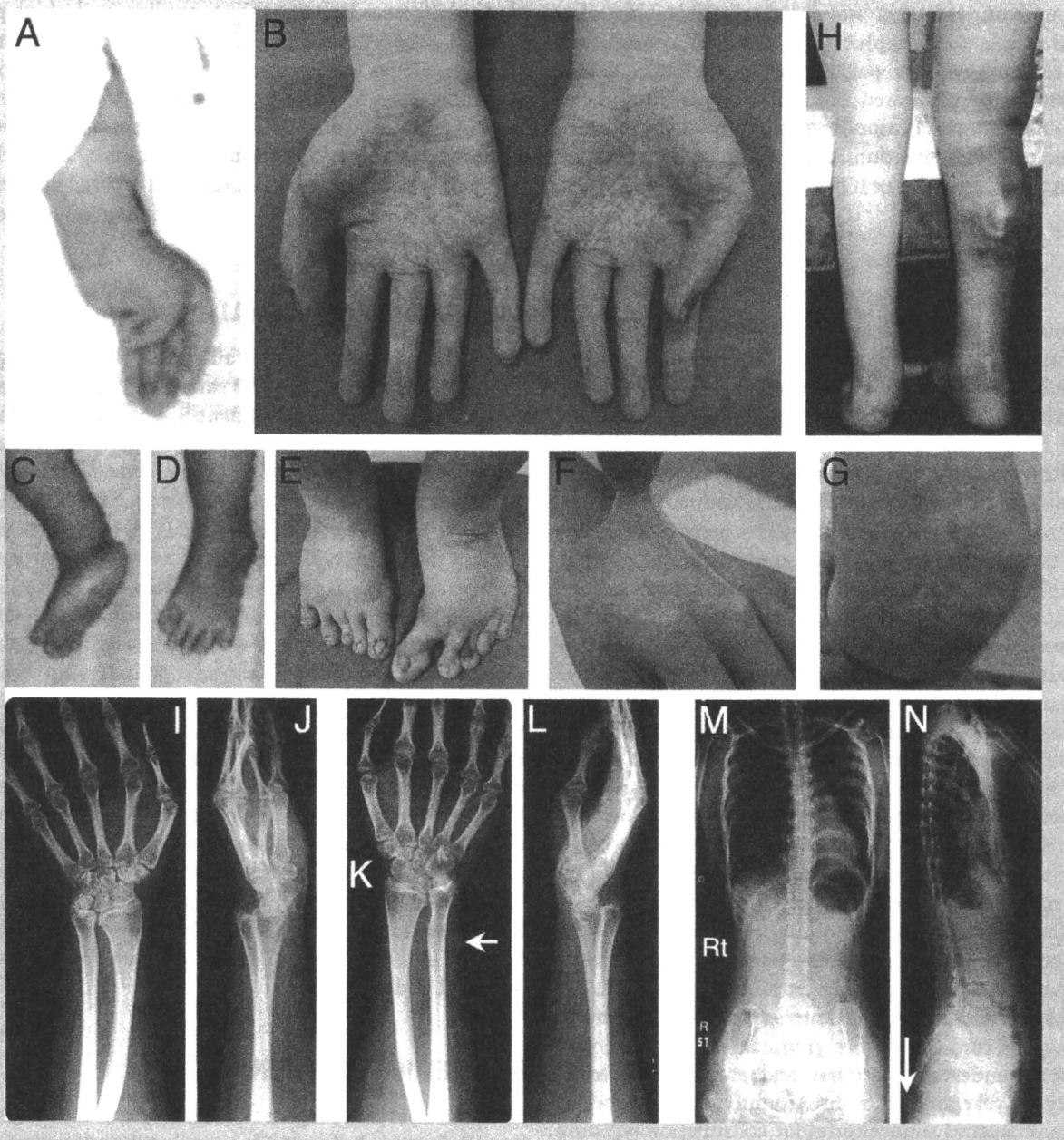

FIG. 6. Patient 5. Clinical photographs of the left hand at age 1 month (A); the hands at age 19 years (B); the right (C) and the left (D) feet at age 1 month; the feet at age 19 years (E); the skin on the back of the left hand at age 19 years (F); the left elbow at age 19 years (G); and a massive subcutaneous hematoma at age 16 years (H). Radiographs of the left (I,J) and the right (K,L) hands, and the spine (M,N) at age 19 years. Arrows indicate ectipic calcification (K,N). [Color figure can be viewed in the online issue, which is available at www.interscience.wiley.com.]

from infectious endocarditis, treated with surgical resection of vegetations and long-term administration of antibiotics. Menstruation, beginning at age 14 years, was irregular. She developed a massive subcutaneous hematoma in the right calf at age 16 years (Fig. 6H), and over the skull after a mild injury at age 17 years, necessitating admission in an ICU and transfusion of packed red cells. She frequently had subcutaneous infections with fistula formation at the elbows and the buttocks, treated with intravenous administration of antibiotics.

When seen by us at age 19 years, her weight was 47 kg (−0.8 SD) and height 158.5 cm (−0.1 SD). She had a slightly asymmetric and slender face with hypertelorism, blue sclerae, strabismus, a short nose with a hypoplastic columella, low-set ears, a small mouth, a high and narrow palate, crowded teeth, and a mildly protruding jaw. She had pectus excavatum, cylindrical fingers with hyperextensibility and flexion-adduction contractures of bilateral thumbs (Fig. 6B), chronic dislocations of bilateral distal radioulnar joints and radial heads, and talipes valgus and planus with

extremely soft subcutaneous tissues at the heels (Fig. 6E), causing difficulty in walking. Her skin was hyperextensible (Fig. 6F), bruisable, and fragile with atrophic scars (Fig. 6G); and showed hyperalgesia to pressure. Fine palmar creases were also noted. Cardiac ultrasonography showed both aortic and mitral valve regurgitation. Abdominal ultrasonography showed nephrolithiasis. Ophthalmological examinations showed myopia and astigmatism, as well as a mild elevation of IOP accompanied by mild visual field loss.

Patient 6

The patient, now a 4-year-old Japanese girl, was the first child of a healthy mother and a healthy non-consanguineous father, both 29 years of age. She was born by vaginal delivery with minimal labor induction at 41 weeks and 5 days of gestation. Her birth weight was 3,004 g (−0.5 SD), length 48.0 cm (−1.2 SD), and OFC 33.0 cm (−0.6 SD). She was admitted in a neonatal ICU for the evaluation and treatment of orthopedic complications, including flexion-adduction contractures of bilateral thumbs, extension contractures of bilateral index to little fingers, flexion contractures of bilateral wrists, rigidity of bilateral hip joints, and bilateral talipes equinovarus. A large anterior fontanelle and diastasis recti with an umbilical hernia were also noted. She showed no spontaneous defecation and required a laxative suppository every day. Her initial clinical diagnosis was Freeman–Sheldon syndrome. Bilateral talipes equinovarus and finger-wrist contractures were treated with serial plaster casts, followed by a surgical correction of the left talipes equinovarus at age 1 year. Atrophy of the flexor hallucis longus muscle was noted. Skin fragility was noticed at the operation, and she was suspected to have EDS. She raised her head at age 5 months, sat unassisted and rolled over at age 9 months, and walked independently at age 1 year and 5 months. Developmental quotient at age 10 months was 64 in physical/motor, 100 in manipulation, 82 in receptive language, 55 in expressive language, 100 in social relationships with adults, and 100 in feeding. Brain and spine MRI, for evaluating delayed closure of the anterior fontanelle, showed tethering of a spinal cord at L3-4 level (normal, L1-2) at age 1 year and 6 months. She underwent duraplasty and resection of protruded coccyges at age 1 year and 11 months. Around age 3 years, she did not need to have laxative suppositories for constipation but only oral magnesium oxide. At age 3 years and 1 month, a subcutaneous cyst appeared at the sacral region, which was resected surgically. At age 3 years and 11 months, a sacral abscess occurred and was treated with surgical drainage, followed by recurrent subcutaneous infections and fistula formation. Two calcified nodules were detected in the abscess. Ophthalmological examinations showed bilateral decreased visual acuity, myopia, astigmatism, and elevated IOP (26 mmHg in the right eye; 29 mmHg in the left), treated with topical administration of a beta-adrenergic receptor blocker (carteolol). Otological examinations showed mild hearing impairment of high-pitched sound with a threshold of 30 dB at 1 kHz and 40 dB at 4 kHz.

When seen by us at age 4 years, her weight was 13.0 kg (−1.3 SD), height 96.2 cm (−1.2 SD), and OFC 49.0 cm (−0.9 SD). Her facial characteristics included hypertelorism, blue sclerae, strabismus, short palpebral fissures, a short and depressed nose with a hypoplastic columella, low-set and rotated ears, redundant cheeks, a long philtrum, a thin upper lip vermilion, and a high palate. Her skin was hyperextensible (Fig. 7D) and bruisable, but only one traumatic would was noticed with an atrophic scar. She had fine palmer creases of hands and could not flex or extend the DIP joints in all fingers (Fig. 7A,B). She had talipes planus, slender and immobile toes, and soft subcutaneous tissues at the heels (Fig. 7C). A mild pectus excavatum and widely spaced nipples were also observed. She hated to be hugged tightly, suggesting hyperalgesia to pressure.

RADIOLOGICAL EXAMINATIONS

Radiographs of hands were available in Patient 1 at age 16 years (Fig. 1O), Patient 2 at age 28 years (Fig. 2L,M), Patient 3 at age 31 years (Fig. 4L,M), and Patient 5 at age 19 years (Fig. 6I–L). Diaphyseal narrowing of the phalanges and metacarpals, and dislocations of bilateral distal radio-ulnar joints were noted. Radiographs of feet were available in Patient 1 at age 16 years (Fig. 1P), Patient 2 at age 28 years (Fig. 2N), and Patient 6 at age 4 years (Fig. 7E–H). Talipes valgus and planus or cavum, with diaphysial narrowing of the phalanges and metatarsals, were noted. Radiographs of spines were available in all patients. Variable degrees of scoliosis or kyphoscoliosis and decreased physiological kyphosis of thoracic spines with tall vertebral bodies were noted: Patient 1 at age 16 years (Fig. 1Q,R; scoliosis with a Cobb angle of 32° at T12-L4, kyphosis with a kyphotic angle of 72° at T11-L3), Patient 2 at age 28 years (Fig. 2O,P; scoliosis with a Cobb angle of 27° at C7-T8, 20° at T8-T12, 15° at T12-L4), Patient 3 at age 31 years (Fig. 4N; scoliosis with a Cobb angle of 8° at T4-T12 and 6° at T12-L4), Patient 4 at age 31 years (Fig. 5; scoliosis with a Cobb angle, of 10° at T1-T10), Patient 5 at age 19 years (Fig. 6M,N; scoliosis with a Cobb angle of 12° at T3-T11), and Patient 6 at age 2 years (Fig. 7I,J; scoliosis with a Cobb angle of 6° at T5-L2). Ectopic calcification was noted in Patients 2 and 5 (Figs. 2M and 6K,N).

BIOCHEMICAL SCREENING

Biosynthesis of procollagens I and III on cultured dermal fibroblasts from Patients 1, 3, 5, and 6 was analyzed as described previously [Hata et al., 1988]. Fibroblasts of all four patients showed normal production of type I and type III procollagens (data not shown), excluding vascular type EDS.

Urinary pyridinoline and deoxypyridinoline excretion was evaluated with HPLC in Patients 1 and 5 as described previously [Pasquali, 1994; Steinmann, 1995]. Normal deoxypyridinoline to pyridinoline ratio was observed in both patients (data not shown), excluding kyphoscoliosis type EDS.

GENETIC SCREENING

G-banded chromosomes were normal in Patients 1, 2, and 6. Direct sequencing of *TGFBR1* and *TGFBR2*, according to the method by Sakai et al. [2006], showed no mutation in Patients 1 and 2.

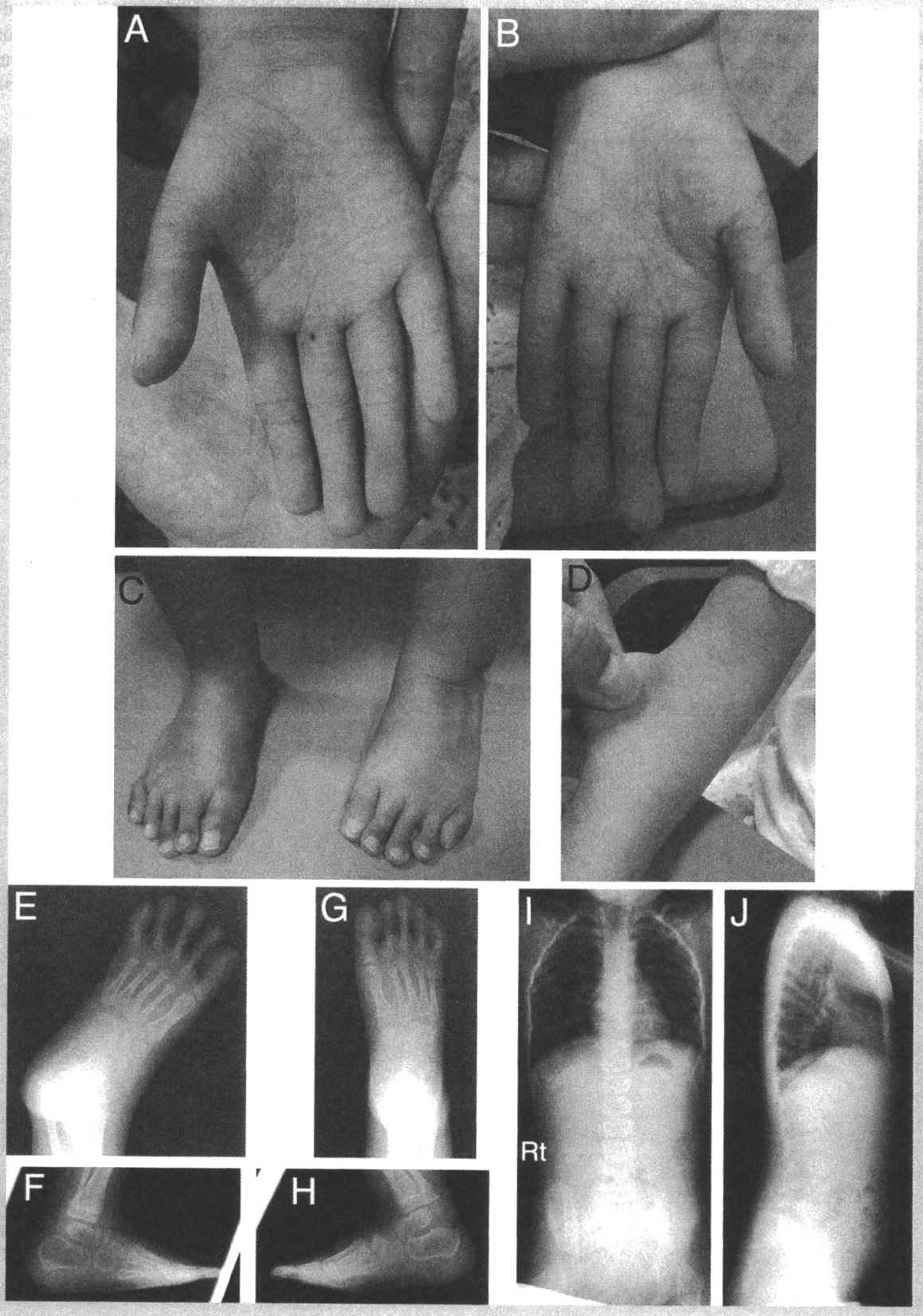

FIG. 7. Patient 6. Clinical photographs, at age 4 years, of the right (A) and the left (B) hands; the feet (C); and the skin on the right forearm (D). Radiographs of the left (E,F) and the right (G,H) feet at age 4 years and the spine at age 2 years (I,J). [Color figure can be viewed in the online issue, which is available at www.interscience.wiley.com.]

DISCUSSION

Clinical features of the six patients are summarized in Table I. Strikingly similar manifestations occur according to the ages, including: (1) *Craniofacial*: large fontanelle, hypertelorism, short and downslanting palpebral fissures, blue sclerae, short nose with hypoplastic columella, low-set and rotated ears, high palate, long philtrum, thin upper lip vermilion, small mouth, and micro-retrognathia in infancy; slender and asymmetric face with protruding jaw from adolescence; (2) *Skeletal*: congenital

TABLE I. Clinical Features of the Six Patients

	Patient 1	Patient 2	Patient 3	Patient 4	Patient 5	Patient 6
Age (years)/sex	16/F	32/F	32/M	32/M	20/F	4/F
Consanguinity	−	+	+	NI	−	−
Craniofacial						
Large fontanelle in infancy	+	+	+	NI	+	+
Hypertelorism	+	+	+	+	+	+
Blue sclerae	+	+	+	+	+	+
Short nose with hypoplastic columella	+	+	+	NI	+	+
Low-set ears	+	+	+	NI	+	+
High-arched palate	+	+	+	+	+	+
Long philtrum and thin upper lip	+	+	+	NI	+	+
Small mouth/micro-retrognathia in infancy	+	+	+	NI	+	NI
Slender face/protruding jaw from adolescence	+	+	+	+	+	NI
Facial asymmetricity from adolescence	+	+	+	+	+	NI
Skeletal						
Congenital multiple contractures	+	+	+	NI	+	+
Tendon abnormalities	+	+	+	NI	+	NI
Recurrent joint dislocations	+	+	+	−	+	−
Pectus deformities	Excavatum	Flat, thin	Flat, thin	Excavatum	Excavatum	Excavatum
Spinal deformities	Kyphoscoliosis	Scoliosis	Kyphoscoliosis	Kyphoscoliosis	Scoliosis	Scoliosis
Slender and/or cylindrical fingers	+	+	+	+	+	+
Progressive talipes deformities	Planus, valgus	Cavus, valgus	Planus, valgus	Planus, valgus	Planus, valgus	Planus
Skin						
Hyperextensibility	+	+	+	+	+	+
Bruisability	+	+	+	+	+	+
Fragility (atrophic scars)	+	+	+	−	+	+
Hyperalgesia to pressure	+	+	+	−	+	+
Fine/acrogeria-like palmar creases	+	+	+	+	+	+
Recurrent subcutaneous infections/fistula formation	+	+	+	−	+	+
Cardiovascular						
Valve abnormalities	ASD, TR, TVP, MVP	−	AR, MR	−	AR, MR, IE	NI
Large subcutaneous hematomas	+	+	+	+	+	−
Respiratory						
(Hemo) pneumothorax	−	+	+	+	−	−
Gastrointestinal						
Constipation	+	+	+	−	+	+
Diverticular perforation	−	+	+	−	−	−
Ophthalmological						
Strabismus	+	+	+	−	+	+
Glaucoma	−	+	−	−	+	+
Refractive errors	Hyperopia	Myopia Astigmatism	Myopia Astigmatism	−	Myopia Astigmatism	Myopia Astigmatism
Hearing impairment	+	+	+	−	−	+
Motor function						
Gross motor developmental delay	+	+	+	NI	+	+

Patients 1 and 2 were reported by Kosho et al. [2005] and Patient 4 was reported by Yasui et al. [2003].
F, female; M, male; −, absent; +: present; NI, no information available; ASD, atrial septal defect; TR, tricuspid valve regurgitation; TVP, tricuspid valve prolapse; MVP, mitral valve prolapse; AR, aortic valve regurgitation; MR, mitral valve regurgitation; IE, infectious endocarditis.

contractures of fingers, wrists, hips, and feet (talipes equinovarus) with anomalous insertions of flexor muscles; progressive joint laxity with recurrent dislocations; slender and/or cylindrical fingers and progressive talipes valgus and cavum or planus, with diaphyseal narrowing of the phalanges, metacarpals, and metatarsals; inability to move fingers and toes separately or smoothly; pectus deformities (flat or excavated); scoliosis or kyphoscoliosis with decreased physiological curvatures of thoracic spines and tall vertebrae; (3) *Cutaneous*: progressive hyperextensibility, bruisability, and fragility with atrophic scars; fine palmar creases from childhood to adolescence and prominent palmar wrinkles showing acrogeria in adulthood; recurrent subcutaneous infections with fistula formation; (4) *Cardiovascular*: cardiac valve abnormalities; recurrent large subcutaneous hematomas from childhood; (5) *Gastrointestinal*: constipation, diverticula perforation; (6) *Respiratory*: (hemo) pneumothorax; (7) *Ophthalmological*: strabismus, glaucoma, refractive errors. Hearing impairment of high-pitched sounds and gross developmental delay are also frequent. Initial diagnosis was Freeman–Sheldon syndrome in Patients 2 and 6, arthrogryposis in Patient 3, and EDS in the others, according to predominant manifestations with ages. In view of these findings, it is reasonable to consider that the patients would share a single disorder consisting of four clinical elements: craniofacial characteristics, congenital multiple contractures, progressive joint and skin laxity, and progressive multisystem tissue fragility. Parental consanguinity in two patients suggested an autosomal recessive mode of inheritance.

The disorder shows all hallmarks of EDS, which are skin hyperextensibility, joint hypermobility, and tissue fragility affecting skin, ligaments, joints, blood vessels, and internal organs [Steinmann et al., 2002]. Characteristic faces are noted in vascular type (thin, delicate, and pinched nose; thin lips; tight skin; hollow cheeks; prominent staring eyes; and tight, firm, lobeless ears) [Beighton et al., 1998; Steinmann et al., 2002], dermatosparaxis type (puffy eyelids with excessive periorbital skin, and large fontanelle) [Steinmann et al., 2002], progenoid form (frontal bossing, sparse scalp hair, prominent eyes, down-slanting palpebral fissures, midface hypoplasia, and small mouth) [Faiyaz-Ul-Haque et al., 2004], and EDS-like spondylocheirodysplasia (down-slanting palpebral fissures, protruding eyes, and blue sclerae) [Giunta et al., 2008], all of which could be distinguishable from our series. Congenital contractures are noted in vascular type (talipes equinovarus), kyphoscoliosis type (talipes equinovarus), arthrochalasia type (hip dislocation) [Beighton et al., 1998; Steinmann et al., 2002], and EDS-like spondylocheirodysplasia (finger contractures and talipes equinovarus) [Giunta et al., 2008]; but distinct finger-wrist contractures or progressive talipes valgus and cavum or planus after corrections of equinovarus, observed in our series, have not been described. Spinal deformities are noted in kyphoscoliosis type (kyphoscoliosis), arthrochalasia type (kyphoscoliosis) [Beighton et al., 1998; Steinmann et al., 2002], and EDS-like spondylocheirodysplasia (platyspondyly, osteopenia, and irregular endplates) [Giunta et al., 2008], whereas decreased physiological curvatures of thoracic spines and tall vertebrae have not been described. Skin hyperextensibility, bruisability, and fragility with atrophic scars in our series were similar to classical type, kyphoscoliosis type, and arthrochalasia type [Beighton et al., 1998; Steinmann et al., 2002], but prominent palmar wrinkles in our adult patients have not been described in previous EDS types. Recurrent large subcutaneous hematomas, occurring after childhood, were the most serious complications in our series, which could have been fatal if the treatment (transfusion of packed red cells or emergency surgical drainage) had been delayed. Superficial or intramuscular small arteries were supposed to be ruptured after minor injuries, followed by acute spread of hemorrhage because of markedly loose subcutaneous tissue. Arterial lesions (dissection, aneurysm, and rupture) are the most important complications in vascular type and occasional but the major life-threatening complications in kyphoscoliosis type. However, aorta, branches of aorta, and major arteries in limbs have been affected in vascular type [Oderich et al., 2005]; and aorta and medium-sized arteries (middle cerebral artery, vertebral artery, femoral artery, and intrathoracic artery) have been affected in kyphoscoliosis type [Wenstrup et al., 1989; Steinmann et al., 2002; Yeowell and Steinmann, 2008]. Normal production of type I and III procollagen excluded vascular type and normal urinary deoxypyridinoline to pyridinoline ratio evaluated with HPLC excluded kyphoscoliosis type. Furthermore, this condition is distinguishable to other connective tissue disorders such as Marfan syndrome (MFS) [Dietz, 2009] and Loeys–Dietz syndrome (LDS) [Loeys and Dietz, 2008]. Although *FBN1* molecular analysis was not performed in our series, distinct facial characteristics and profound skin and joint laxity as well as other serious multisystem complications have never been reported in MFS. No mutation in *TGFBR1* or *TGFBR2* excluded LDS.

Present patients shared many clinical features with a Pakistani sister and brother reported by Steinmann et al., [1975], including characteristic face (a slender and asymmetric face with hypertelorism, downslanting palpebral fissures, blue sclerae, a short nose with a hypoplastic columella, a high palate, a long philtrum, and a small mouth in the brother at age 18 years); talipes equinovarus and progressive talipes vagus and planus after corrections; joint laxity; scoliosis or kyphoscoliosis with tall vertebral bodies; arachnodactyly with diaphysial narrowing of phalanges, metacarpals, and metatarsals; skin hyperextensibility, bruisability, and fragility with atrophic scars; hyperalgesia to pressure; and delayed motor development. The sibs have been classified into a subtype of kyphoscoliosis type EDS [Steinmann et al., 2002], though lysyl hydroxylase activity was proved to be normal [Wenstrup et al., 1989].

In conclusion, we propose that these present patients represent a new clinically recognizable type of EDS characterized by distinct craniofacial features, multiple congenital contractures, progressive joint and skin laxity, and progressive multisystem fragility-related manifestations, including recurrent large subcutaneous hematomas and other cardiac, respiratory, gastrointestinal, ophthalmological complications.

ACKNOWLEDGMENTS

We express gratitude to all the patients and their families who participated in this study. We also thank Dr. Y. Seta, Dr. Y. Toki, Dr. T. Miyamoto, Dr. K. Arai, Dr. F. Miura, Dr. H. Ikei, Dr. N. Hoshino, Dr. T. Muneta, Dr. N. Kurosawa, Dr. M. Nagasaka, and Dr. M. Kato for contribution of patients' information and samples. This work was supported by Research on Intractable Diseases from Japanese Ministry of Health, Welfare, and Labor (#2141039040)

(T.K., A.H., Y.F., and N.M.); Shinshu Association for the Advancement of Medical Sciences (T.K.); and Grant-in-Aid for Exploratory Research of Young Scientists, Shinshu University (T.K.).

REFERENCES

Abu A, Frydman M, Marek D, Pras E, Nir U, Reznik-Wolf H, Pras E. 2008. Deleterious mutations in the zinc-finger 469 gene cause brittle cornea syndrome. Am J Hum Genet 82:1217–1222.

Beighton P, De Paepe A, Steinmann B, Tsipouras P, Wenstrup R. 1998. Ehlers-Danlos syndromes: Revised nosology, Villefranche, 1997. Am J Med Genet 77:31–37.

Dietz HC. 2009. Marfan syndrome. In: GeneReviews at genetests: Medical Genetics Information Resource (database online).Copyright, University of Washington. Seattle: 1997–2009. Available at http://www.genetests.org. Accessed April 11, 2010.

Faiyaz-Ul-Haque M, Zaidi SHE, Al-Ali M, Al-Mureikhi MS, Kennedy S, Al-Thani G, Tsui LC, Teebi AS. 2004. A novel missense mutation in the galactosyltransferase-I (*B4GALT7*) gene in a family exhibiting facioskeletal anomalies and Ehlers-Danlos syndrome resembling the progeroid type. Am J Med Genet Part A 128A:39–45.

Giunta C, Elcioglu NH, Albrecht B, Eich G, Chambaz C, Janecke A, Yeowell H, Weis MA, Eyre DR, Kraenzlin M, Steinmann B. 2008. Spondylocheiro dysplastic form of the Ehlers-Danlos syndrome-an autosomal recessive entity caused by mutations in the zinc transporter gene SLC39A13. Am J Hum Genet 82:1290–1305.

Hata R, Kurata S, Shinkai H. 1988. Existence of malfunctioning pro alpha 2(I) collagen genes in a patient with pro alpha 2(I)-chain-defective variant of Ehlers-Danlos syndrome. Eur J Biochem 174:231–237.

Kosho T, Takahashi J, Ohashi H, Nishimura G, Kato H, Fukushima Y. 2005. Ehlers-Danlos syndrome type VIB with characteristic facies, decreased curvatures of the spinal column, and joint contractures in two unrelated girls. Am J Med Genet Part A 138A:282–287.

Kresse H, Rosthoj S, Quentin E, Hollmann J, Glossl J, Okada S, Tonnesen T. 1987. Am J Hum Genet 41:436–453.

Loeys BL, Dietz HC, 2008. Loeys-Dietz syndrome. In: GeneReviews at genetests: Medical Genetics Information Resource (database online). Copyright, University of Washington, Seattle 1997–2009. Available at http: //www.genetests.org. Accessed April 11, 2010.

Mao JR, Bristow J. 2001. The Ehlers-Danlos syndrome: On beyond collagens. J Clin Invest 107:1063–1069.

Oderich GS, Panneton JM, Bower TC, Lindor NM, Cherry KJ, Noel AA, Kalra M, Sullivan T, Gloviczki P. 2005. The spectrum, management and clinical outcome of Ehlers-Danlos syndrome type IV: A 30-year experience. J Vasc Surg 42:98–106.

Pasquali M. 1994. Urinary pyridinium cross-links: A non invasive diagnostic test for Ehlers-Danlos syndrome type VI. N Engl J Med 331: 132–133.

Sakai H, Visser R, Ikegawa S, Ito E, Numabe H, Watanabe Y, Mikami H, Kondoh T, Kitoh H, Sugiyama R, Okamoto N, Ogata T, Fodde R, Mizuno S, Takamura K, Egashira M, Sasaki N, Watanabe S, Nishimaki S, Takada F, Nagai T, Okada Y, Aoka Y, Yasuda K, Iwasa M, Kogaki S, Harada N, Mizuguchi T, Matsumoto N. 2006. Comprehensive genetic analysis of relevant four genes in 49 patients with Marfan syndrome or Marfan-related phenotypes. Am J Med Genet Part A 140A:1719–1725.

Schalkwijk J, Zweers MC, Steijlen PM, Dean WB, Taylor G, van Vlijmen IM, van Haren B, Miller WL, Bristow J. 2001. A recessive form of the Ehlers-Danlos syndrome caused by tenascin-X deficiency. N Engl J Med 345:1167–1175.

Schwarze U, Hata R, McKusick VA, Shinkai H, Hoyme HE, Pyeritz RE, Byers PH. 2004. Rare autosomal recessive cardiac valvular form of Ehlers-Danlos syndrome results from mutations in the COL1A2 gene that activate the nonsense-mediated RNA decay pathway. Am J Hum Genet 74:917–930.

Steinmann B. 1995. Urinary pyridinoline cross-links in Ehlers-Danlos syndrome type VI. Am J Hum Genet 57:1505–1508.

Steinmann B, Gitzelmann R, Vogel A, Grant ME, Harwood R, Sear CHJ. 1975. Ehlers-Danlos syndrome in two siblings with deficient lysyl hydroxylase activity in cultured skin fibroblasts but only mild hydroxylysine deficit in skin. Helv Paediat Acta 30:255–274.

Steinmann B, Royce PM, Superti-Furga A. 2002. The Ehlers-Danlos syndrome. In: Royce PM, Steinmann B, editors. Connective tissue and its heritable disorders. New York: Wiley-Liss. pp. 431–523.

Wenstrup RJ, Murad S, Pinnell SR. 1989. Ehlers-Danlos syndrome typw IV: Clinical manifestations of collagen lysyl hydroxylase deficiency. J Pediatr 115:405–409.

Yasui H, Adachi Y, Minami T, Ishida T, Kato Y, Imai K. 2003. Combination therapy of DDAVP and conjugated estrogens for a recurrent large subcutaneous hematoma in Ehlers-Danlos syndrome. Am J Hematol 72:71–72.

Yeowell H, Steinmann B., 2008. Ehlers-Danlos syndrome, kyphoscoliotic form. In: GeneReviews at genetests: Medical Genetics Information Resource (database online).Copyright, University of Washington, Seattle 1997–2009. Available at http: //www.genetests.org. Accessed January 23, 2010.

RESEARCH ARTICLE

Human Mutation

OFFICIAL JOURNAL
HGVS
HUMAN GENOME VARIATION SOCIETY
www.hgvs.org

Loss-of-Function Mutations of *CHST14* in a New Type of Ehlers-Danlos Syndrome

Noriko Miyake,[1*†] Tomoki Kosho,[2†] Shuji Mizumoto,[3†] Tatsuya Furuichi,[4] Atsushi Hatamochi,[5] Yoji Nagashima,[6] Eiichi Arai,[7] Kazuo Takahashi,[8] Rie Kawamura,[2] Keiko Wakui,[2] Jun Takahashi,[9] Hiroyuki Kato,[9] Hiroshi Yasui,[10] Tadao Ishida,[10] Hirofumi Ohashi,[11] Gen Nishimura,[12] Masaaki Shiina,[13] Hirotomo Saitsu,[1] Yoshinori Tsurusaki,[1] Hiroshi Doi,[1] Yoshimitsu Fukushima,[2] Shiro Ikegawa,[4] Shuhei Yamada,[3] Kazuyuki Sugahara,[3] and Naomichi Matsumoto[1*]

[1]Department of Human Genetics, Yokohama City University Graduate School of Medicine, Yokohama, Japan; [2]Department of Medical Genetics, Shinshu University School of Medicine, Matsumoto, Japan; [3]Laboratory of Proteoglycan Signaling and Therapeutics, Hokkaido University Graduate School of Life Science, Sapporo, Japan; [4]Laboratory for Bone and Joint Disease, Center for Genomic Medicine, RIKEN, Tokyo, Japan; [5]Department of Dermatology, Dokkyo Medical University, School of Medicine, Tochigi, Japan; [6]Department of Molecular Pathology, Yokohama City University Graduate School of Medicine, Yokohama, Japan; [7]Department of Pathology, Saitama Medical University, Saitama, Japan; [8]Department of Environmental Immuno-Dermatology, Yokohama City University Graduate School of Medicine, Yokohama, Japan; [9]Department of Orthopedics, Shinshu University School of Medicine, Matsumoto, Japan; [10]First Department of Internal Medicine, Sapporo Medical University, Sapporo, Japan; [11]Division of Medical Genetics, Saitama Children's Medical Center, Saitama, Japan; [12]Department of Radiology, Tokyo Metropolitan Kiyose Children's Hospital, Tokyo, Japan; [13]Department of Biochemistry, Yokohama City University Graduate School of Medicine, Yokohama, Japan

Communicated by Jürgen Horst

Received 17 March 2010; accepted revised manuscript 24 May 2010.
Published online in Wiley InterScience (www.interscience.wiley.com). DOI 10.1002/humu.21300

ABSTRACT: Ehlers-Danlos syndrome (EDS) is a heterogeneous connective tissue disorder involving skin and joint laxity and tissue fragility. A new type of EDS, similar to kyphoscoliosis type but without lysyl hydroxylase deficiency, has been investigated. We have identified a homozygous *CHST14* (carbohydrate sulfotransferase 14) mutation in the two familial cases and compound heterozygous mutations in four sporadic cases. *CHST14* encodes dermatan 4-*O*-sulfotransferase 1 (D4ST1), which transfers active sulfate from 3′-phosphoadenosine 5′-phosphosulfate to position 4 of the *N*-acetyl-D-galactosamine (GalNAc) residues of dermatan sulfate (DS). Transfection experiments of mutants and enzyme assays using fibroblast lysates of patients showed the loss of D4ST1 activity. *CHST14* mutations altered the glycosaminoglycan (GAG) components in patients' fibroblasts. Interestingly, DS of decorin proteoglycan, a key regulator of collagen fibril assembly, was completely lost and replaced by chondroitin sulfate (CS) in the patients' fibroblasts, leading to decreased flexibility of GAG chains. The loss of the decorin DS proteoglycan due to *CHST14* mutations may preclude proper collagen bundle formation or maintenance of collagen bundles while the sizes and shapes of collagen fibrils are unchanged as observed in the patients' dermal tissues. These findings indicate the important role of decorin DS in the extracellular matrix and a novel pathomechanism in EDS.
Hum Mutat 31:1–9, 2010. © 2010 Wiley-Liss, Inc.

KEY WORDS: Ehlers-Danlos syndrome; EDS; *CHST14*; dermatan sulfate; dermatan 4-*O*-sulfotransferase 1; D4ST1; collagen bundle formation; decorin

Introduction

Ehlers-Danlos syndrome (EDS) is a heterogeneous connective tissue disorder characterized by joint and skin laxity and tissue fragility [Steinmann et al., 2002], affecting as many as 1 in 5,000 individuals. The pathomechanisms of EDS consist of dominant-negative effects of mutant procollagen α-chains, α-chain haploinsufficiency, and deficiency of collagen-processing enzymes [Mao and Bristow, 2001]. In a revised nosology [Beighton et al., 1998], EDS was classified into six major types as well as additional minor forms. We previously described two unrelated patients showing characteristic facial and skeletal features with partial similarity to kyphoscoliosis type EDS but without lysyl hydroxylase deficiency (EDS-VIB) [Kosho et al., 2005]. Through long-term clinical evaluation of them as well as additional four unrelated patients including one reported previously [Yasui et al., 2003], we confirmed that these patients represent a new type of EDS [Kosho et al., 2010]. The evidence that two of six probands were born between consanguineous parents (Fig. 1A) suggests that this disease is inherited in an autosomal recessive fashion. Thus, we performed homozygosity mapping to find the disease-causative gene and successfully identified pathological mutations in the carbohydrate sulfotransferase 14 (*CHST14*: GenBank reference sequence, NM_130468.3) gene, in all six probands. *CHST14* encodes dermatan 4-*O*-sulfotransferase 1 (D4ST1), which transfers active sulfate to the *N*-acetyl-D-galactosamine (GalNAc) residues of dermatan sulfate (DS). Furthermore, we

Additional Supporting Information may be found in the online version of this article.

†The first three authors contributed equally to this article.

*Correspondence to: Noriko Miyake, Department of Human Genetics, Yokohama City University Graduate School of Medicine, 3-9 Fukuura, Kanazawa-ku, Yokohama 236-0004, Japan. E-mail: nmiyake@yokohama-cu.ac.jp or Naomichi Matsumoto, Department of Human Genetics, Yokohama City University Graduate School of Medicine, 3-9 Fukuura, Kanazawa-ku, Yokohama 236-0004, Japan. E-mail: naomat@yokohama-cu.ac.jp

© 2010 WILEY-LISS, INC.

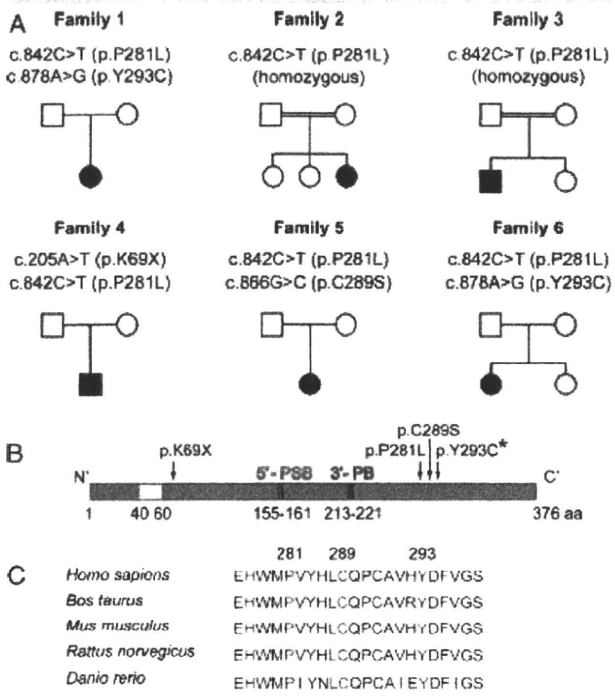

Figure 1. *CHST14* mutations in the patients. **A:** Pedigrees of the patients. Mutations in both alleles were found in all. **B:** A schematic representation of D4ST1 encoded by *CHST14*. Arrows indicate the position of mutations found in the patients. The red and blue boxes indicate a 5′-phosphosulfate binding site (5′-PSB) and a 3′-phosphate binding site (3′-PB), respectively. Light blue, yellow, and purple boxes denote cytoplasmic, transmembrane, and luminal regions, respectively. *p.Y293C (c.878A>G) is the same missense mutation identified in the Japanese ATCS sibs reported [Dündar et al., 2009]. **C:** D4ST1 amino acid alignment for three missense mutations evolutionally conserved.

conducted pathological and glycobiological investigations to reveal the pathomechanism of this disease.

Materials and Methods

Subjects

We analyzed six Japanese patients clinically diagnosed as showing a specific type of EDS [Kosho et al., 2005, 2010] in this study. Briefly, they clinically resemble the kyphoscoliosis type EDS characterized by joint laxity, progressive scoliosis, tissue fragility with atrophic scars, easy bruising, arterial rupture, and Marfanoid habitus. However, the lysyl hydroxylase deficiency, which is the reliable diagnostic test for the kyphoscoliosis type, was not observed in the probands [Kosho et al., 2005, 2010]. One of the authors (T.K.) evaluated all cases. This study was approved by the institutional review boards of Yokohama City University School of Medicine, Shinshu University School of Medicine, and Hokkaido University Graduate School of Advanced Life Science. Informed consent was obtained from all subjects involved in this study.

Mapping and Mutation Analysis

We performed the whole genome linkage analysis using Affymetrix Human Mapping single nucleotide polymorphism (SNP) 10K XbaI 142 2.0 array (Affymetrix, St. Clara, CA) in two affected probands (patients 2 and 3) and six unaffected members from two consanguineous families. Haplotype analysis was performed using seven microsatellite markers (*D15S1002, D15S1007, D15S118, D15S1044, D15S214, D15S978,* and *D15S117*) purchased from Applied Biosystems (Bedford, MA). These markers were designed based on the Marshfield genetic map (http://research.marshfieldclinic.org/genetics). We screened three affected individuals (patients 1, 2, and 3) for mutations in seven genes (*THBS1, FSIP1, VSP39, MEIS2, DLL4, CHAC1,* and *CHST14*) among 109 known genes within the 7.3-Mb candidate locus. After identifying a mutation, we only screened *CHST14* (NM_130468.3) in the remaining individuals (patients 4, 5, and 6). We amplified genomic DNA by PCR using four primer sets (sequences available on request). Nucleotide changes found in the patients were checked in 376 Japanese control samples (752 alleles). Compound heterozygosity was confirmed by direct sequencing of the patients' parents or allele specific sequencing after cloning of respective regions covering two different mutation sites of *CHST14*. Nucleotide numbering reflects cDNA numbering with +1 corresponding to the A of the ATG translation initiation codon in the reference sequence, according to journal guidelines (www.hgvs.org/mutnomen). The initiation codon is codon 1.

Primary Fibroblast Culture

We obtained skin fibroblasts from patient 1 at age 6 years, her mother at 27 years, and patient 3 at 29 years. Their age- and sex-adjusted normal controls (a 6-year-old girl: control 1 and a 36-year-old man: control 2) were purchased from Japan Health Sciences Foundation (http://www.jhsf.or.jp/). Cells were cultured in Dulbecco's modified Eagle's medium with 10% heat-inactivated fetal bovine serum (FBS), 100 U/ml penicillin, 100 U/ml streptomycin, and 2 mM L-glutamine (Invitrogen, Carlsbad, CA).

Sulfotransferase Assays

COS-7 cells transiently transfected with the N′-V5-D4ST1 vectors using FuGENE™ 6 (Roche Diagnostics, Indianapolis, IN) and human fibroblasts were lysed with 200 µl of M-PER® mammalian protein extraction reagent (Thermo Fisher Scientific Inc., Waltham, MA). Sulfotransferase activities of each cell lysate toward dermatan, chemically desulfated DS were assayed as described before [Mikami et al., 2003]. The [^{35}S]sulfate incorporation was quantified by determination of the radioactivity in the flow-through fractions of the gel filtration chromatography by liquid scintillation counting.

Disaccharide Composition Analysis of Chondroitin (CS)/DS Chains Isolated from Fibroblasts

Cell lysates of fibroblasts cultured on 100-mm plates were digested with actinase E (Kaken Pharmaceutical Co., Ltd., Tokyo, Japan) and GAG-peptides were recovered by 80% ethanol as described [Uyama et al., 2006]. After being desalted using a centrifugal filter, Amicon® Ultra-4 (Ultracel-3k, Millipore Corp., Billerica, MA), the GAG-peptides were digested with CSase ABC from *Proteus vulgaris* (EC 4.2.2.20) (Seikagaku Corp., Tokyo, Japan) [Yamagata et al., 1968], a mixture of CSase AC-I from *Flavobacterium heparinum* (EC 4.2.2.5) (Seikagaku Corp.) [Yamagata et al., 1968], and AC-II from *Arthrobacter aurescens* (EC 4.2.2.5) (Seikagaku Corp.) [Hiyama and Okada, 1975], or CSase B from *Flavobacterium heparinum* (EC 4.2.2.19) (IBEX Technologies, Kawasaki, Japan) [Michelacci and Dietrich, 1974]. The digests were labeled with a fluorophore 2-aminobenzamide (2AB) and aliquots

of the 2AB-derivatives of CS/DS oligosaccharides were analyzed by anion-exchange HPLC on a PA-03 column (YMC Co., Kyoto, Japan) as previously described [Kinoshita and Sugahara, 1999].

Immunoblotting

Each cell lysate of COS-7 cells expressing the recombinant N′-V5-D4ST1 was subjected to SDS-PAGE using a 10–20% SDS-polyacrylamide gradient gel. The serum-free conditioned medium from fibroblast cultures was collected and concentrated using Amicon Ultra-4 filters (Ultracel-30k). An aliquot of the sample was digested with CSase ABC, CSase AC, CSase B, or buffer alone, and each digest was subjected to SDS-PAGE using a 7.5% SDS-polyacrylamide gel. Immunoblotting was carried out using anti-V5 antibody (Invitrogen) for D4ST1-transfected cells or antihuman decorin antibody (clone 115402; R&D Systems, Minneapolis, MN) for secreted decorin DS proteoglycan from fibroblasts.

PAI1 and SMAD7 Expression Analysis with TGF-β1 Stimulation

Fibroblasts were grown to 70–80% confluence in 24-well multiplates and transfected with 200 ng of empty, wild-type, or mutant *CHST14* expression vector, using FuGENE 6. At 24 hr after transfection, cells were transferred to low serum medium (0.2% FBS) and, after 8 hr treated with TGF-β1 (1 ng/ml; PeproTech Inc., Rocky Hill, NJ) for 24 hr. Total RNA was extracted using the SV-Total RNA Isolation system (Promega, Madison, WI). Randomly primed cDNA was synthesized using the Taqman Multiscribe Reverse Transcriptase kit (Applied Biosystems). Real-time PCR was carried out on the StepOnePlus Real-Time PCR system (Applied Biosystems) using the QuantiTect SYBR Green PCR kit (Qiagen, Tokyo, Japan). The following primers were used for amplification: *CHST14*, 5′-CTATGA-GAGGCTGGAGGCTG-3′ and 5′-AGGCAAAGAGGGAGAAGTCC-3′; *PAI1*, 5′-CAGACCAAGAGCCTCTCCAC3′ and 5′- GACTGTTCC-TGTGGGGTTGT-3′; *SMAD7*, 5′-TTGCTGTGAATCTTACGGGA-3′ and 5′-CCAGATAATTCGTTCCCCCT-3′; and *GAPDH*, 5′-ACCA-CAGTCCATGCCATCAC-3′ and 5′-TCCACCACCCTGTTGCTGTA-3′.

Reporter Gene Assay

Fibroblasts were grown to 70–80% confluence in 24-well multiplates and transfected with plasmid DNA mixtures using FuGENE 6. The DNA mixture involved 100 ng of SBE4-luc vector, 200 ng of empty, wild-type, or mutant *CHST14* expression vector, and 25 ng of a reference vector, pRL-TK. The SBE4-Luc vector is a TGF-β-responsive reporter containing four tandem copies of a SMAD-binding element (SBE) linked to luciferase [Zawel et al., 1998]. At 24 hr after transfection, cells were transferred to low serum medium (0.2% FBS) and, after 8 hr, treated with TGF-β1 (1 ng/ml) for a further 24 hr. Luciferase activities were measured using the PG-DUAL-SP reporter assay system (Toyo Ink., Tokyo, Japan) and a Lumat LB 9507 luminometer (Berthold Technologies GmbH & Co. KG, Bad Wildbad, Germany). Relative luciferase activity was calculated by normalizing the transfection efficiency of Renilla luciferase activity against the reference vector.

SMAD2 Phosphorylation with TGF-β1 Stimulation

Fibroblasts were grown to 70–80% confluence in six-well multiplates and were transfected with 1.5 μg of empty, wild-type, or mutant *CHST14* expression vector, using FuGENE 6. At 24 hr after transfection, cells was transferred to low serum medium (0.2% FBS) and, after 8 hr, were treated with TGF-β1 (1 ng/ml) for 30 min. Cells were lysed using M-PER protein extraction kits (Pierce, Rockford, IL) containing a protease inhibitor cocktail (Roche Diagnostics). Proteins in the cell lysate were separated on SDS-PAGE gels and electrophoretically transferred to PVDF membranes. After blocking with 5% nonfat dry milk in PBS-Tween, the membranes were incubated first with antibodies against phospho-SMAD2 or SMAD2 (Cell Signaling Technology, Danvers, MA) and then with goat polyclonal antibodies against rabbit IgG conjugated with horseradish peroxidase (Cell Signaling Technology). Band intensities were measured using ImageJ software (http://rsbweb.nih.gov/ij/).

Pathology

Skin specimens were obtained from the upper arms of patients 5 and 6. For light microscopy using a BX51 microscope (Olympus, Tokyo, Japan), skin specimens were fixed with 20% buffered neutral formalin solution and 3–5-μm sections were stained with H&E. For transmission electron microscopy, skin specimens were fixed in 2.5% glutaraldehyde for 2 hr, postfixed in 1% osmium tetroxide for 2 hr, dehydrated in a graded ethanol series, and embedded in epoxy resin (Epon 812, TAAB, Berks, UK). Semithin sections (4 μm) were stained with toluidine blue. Ultrathin sections (100 nm) were stained with uranyl acetate and lead citrate and examined with a transmission electron microscope (JEM-1011, JEOL Ltd., Tokyo, Japan).

Statistical Analyses

All values are described as mean ± SEM. Where appropriate, we assessed between-groups effects by unpaired *t* tests for two groups and ANOVA with Dunnett's adjustment for more than two groups using GraphPad Prism 5 for Windows, version 5.02 (www.graphpad.com).

The detailed methods are described in the Supp. Methods.

Results

Genetic Analysis

We performed homozygosity mapping of two independent consanguineous families (families 2 and 3) and identified the largest 8.15-Mb homozygous region at chromosome 15q14–q15.3 with the maximum LOD Score 2.885, and by using additional microsatellite markers narrowed it down to a 7.3-Mb region (Supp. Fig. S1). Among 109 known genes within this region, the *CHST14* gene (encoding D4ST1) harbored the same homozygous missense mutation (c.842C>T: p.P281L) in the two families and compound heterozygous mutations in the other four (Fig. 1A and B). Mutations include one nonsense (c.205A>T: p.K69X) and three missense mutations (c.842C>T: p.P281L, c.866G>C: p.C289S, and c.878A>G: p.Y293C) occurring at evolutionally conserved amino acids (Fig. 1C). They were absent in 376 Japanese normal controls.

Sulfotransferase Activity

D4ST1 transfers a sulfate group from 3′-phosphoadenosine 5′-phosphosulfate to position 4 of the *N*-acetyl-D-galactosamine (GalNAc) residues of DS, which is abundantly expressed in skin, aortic wall, tendon, and bone [Penc et al., 1998]. Mutant D4ST1 proteins showed significantly decreased sulfotransferase activity towards dermatan (Fig. 2A) regardless of similar expression levels (Fig. 2B). The sulfotransferase activity was also measured in the

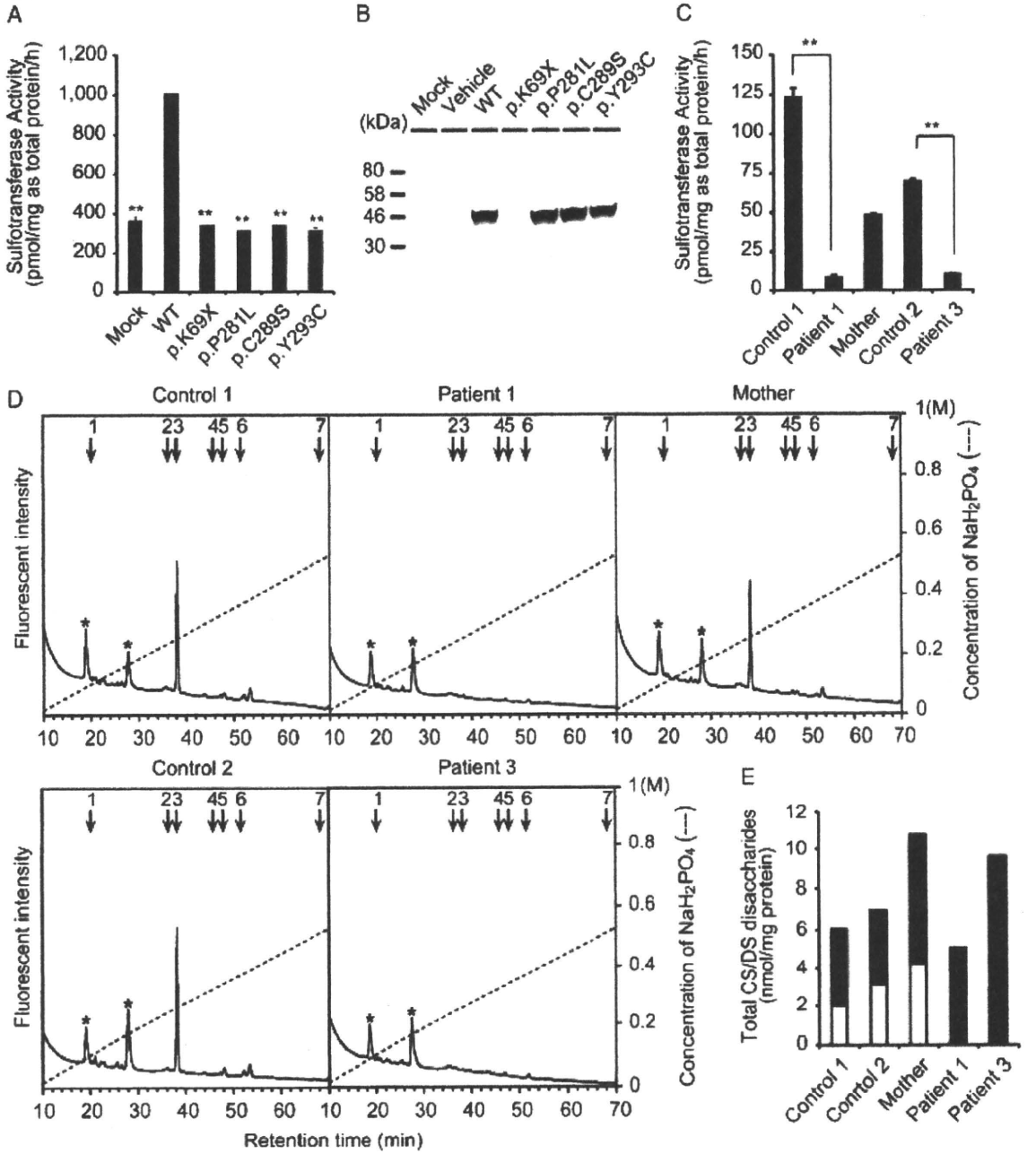

Figure 2. Glycobiological studies. **A:** Sulfotransferase activity of the recombinant D4ST1 of a control and four mutant forms: p.K69X, p.P281L, p.C289S, and p.Y293C. The activity is shown as the incorporation of [^{35}S]SO_4 from the donor [^{35}S]PAPS into the acceptor dermatan. Values are the mean ± SEM ($n = 3$) $^{**}P < 0.0001$ versus WT by one-way ANOVA with Dunnett's adjustment. **B:** Immunoblotting for the exogenous D4ST1 expression in COS-7 cell using the anti-V5 antibody. The mutant p.K69X was too small to be detected (predicted to be approximately 11 kDa). **C:** Sulfotransferase activity toward dermatan in the skin fibroblasts derived from patients 1 and 3, mother of patient 1, and sex- and age-matched healthy controls (controls 1 and 2 for patients 1 and 2, respectively) (mean ± SEM, $n = 3$). $^{**}P < 0.0001$ by two-tailed unpaired t test. **D:** Anion-exchange chromatograms of DS disaccharides obtained by CSase B digestion of GAG-peptides from the skin fibroblasts. The elution positions of authentic 2AB-labeled disaccharide standards are indicated by numbered arrows. 1, ΔHexUA-GalNAc; 2, ΔHexUA-GalNAc(6S); 3, ΔHexUA-GalNAc(4S); 4 ΔHexUA(2S)-GalNAc(6S); 5, ΔHexUA(2S)-GalNAc(4S); 6, ΔHexUA-GalNAc(4S,6S), and 7, ΔHexUA(2S)-GalNAc(4S,6S). Asterisks indicate impurities. **E:** The total amounts of CS and DS derived from skin fibroblasts. The total disaccharide contents of CS (black box) and DS (white box) were calculated based on the peak areas in the chromatograms of the digests with CSase AC and CSase B, respectively.

lysates of primary fibroblasts. The mean activity of the fibroblast lysates of the patients was significantly decreased to 6.7% (patient 1) and 14.5% (patient 3) of each age- and sex-matched control 1 and 2, respectively (Fig. 2C). These data indicate mutations in this study result in loss of function.

Glycosaminoglycan (GAG) Chain Analysis

The disaccharide compositions of DS and chondroitin sulfate (CS) in fibroblasts derived from patients and controls were analyzed by anion-exchange HPLC after digestion with